A study on the sorption mechanism of Au and Pt complex anions on δ-MnO2: A geochemical model reaction to elucidate the concentration of Au and Pt into marine ferromanganese crust

前野, 真実子

https://doi.org/10.15017/1441033

出版情報：九州大学, 2013, 博士（理学）, 課程博士
バージョン：
権利関係：全文ファイル公表済

A study on the sorption mechanism of Au and Pt complex anions on δ-MnO_2:

A geochemical model reaction to elucidate the concentration of Au and Pt into marine ferromanganese crust

前野　真実子

Contents

Chapter I General introduction

I-1 Background of thesis 1

I-2 Purpose of thesis 12

References 14

Chapter II Sorption mechanism of Pt(II) complex anion on manganese dioxide (δ-MnO_2) and their spontaneous oxidation to Pt(IV)

II-1 Introduction 16

II-2 Experimental 18

II-3 Results and Discussion 22

References 39

Chapter III Simultaneus sorption of Pt(II) and Au(III) complex anions on manganese dioxide (δ-MnO_2) and their coupled redox behavior

III-1 Introduction 42

III-2 Experimental 46

III-3 Results and Discussion 49

References 64

Chapter IV Conclusion and geochemical implication 67

References 73

Acknowledgements 74

Chapter I
General introduction

I-1 Background of thesis

I-1-1 What is ferromanganese crust?

Ferromanganese oxide widely distributes as aggregate of black blocks near surface of seabed. The spherical block is called “nodule”. On the other hand, ferromanganese oxide which covers on the surface of rock near the top of seamount is called “crust”. The both nodule and crust are black or burnt umber. They seem to be apparently uniform, however show complicated structure under observation by microscope. A piece of igneous or sedimentary rocks is often found near the center of nodules. The piece of rocks may play a role as nuclei for growth site of ferromanganese nodule. While, ferromanganese crust covers on the basement rock of seamount. Major constituents of ferromanganese nodule and crust are fine particles of hydrous ferric and manganese oxides with size of 0.1 to 0.01 μm whose crystallinity is low. The nodule and crust are porous and the permeability attains to 40 to 60 %. During the growth, the ferromanganese nodule and crust take up a piece of rocks with various sizes, dead bodies of living things, cosmic dust etc. As a result, the complex fine texture is formed as described above. Interestingly, some metals are specifically concentrated into ferromanganese nodule and crust from seawater. The average content of more than twenty elements such as Cu, Ni, Co, Si, Al exceeds 0.1 %. Therefore, ferromanganese nodule and crust are called “poly metallic oxide” as another name.

I-1-2 Chemical state of manganese and iron in seawater

Figure I-1 shows the vertical concentration distribution for manganese and iron in ocean. Manganese and iron are major elements of marine ferromanganese nodule and crust. In Fig. I-1, the vertical concentration distribution for dissolved oxygen in ocean is also shown (Nozaki, 1992). Manganese and iron, which are necessary for the formation of ferromanganese nodule and crust, are supplied from chemical weathering of rocks on land, chemical weathering of oceanic crust, hydrothermal fluid from seabed etc. Manganese and iron are present as fine particles of Mn(IV) and Fe(III) hydrous oxides (sinking particle) in seawater that is shallower than 1000 m. In the distribution of dissolved oxygen, its concentration shows minimum around 1000 m depth (oxygen minimum zone). In the Eh-pH diagram, the boundary between Mn(II) and Mn(IV) is present in the variable region of redox potential in ocean, indicating that the chemical state of manganese ion can easily convert between Mn(II) and Mn(IV) depending on the dissolved oxygen concentration. The idea is supported by the opposite correlation between the vertical concentration distribution of manganese and dissolved oxygen. However, there is no clear correlation between the vertical concentration distributions of iron and dissolved oxygen. Judging from the difference of sensitivity for redox potential between manganese and iron, the behavior of manganese and iron is considered to be different in ocean. Based on the difference between the behaviors of manganese and iron, the formation process of ferromanganese nodule and crust is discussed in the next section.

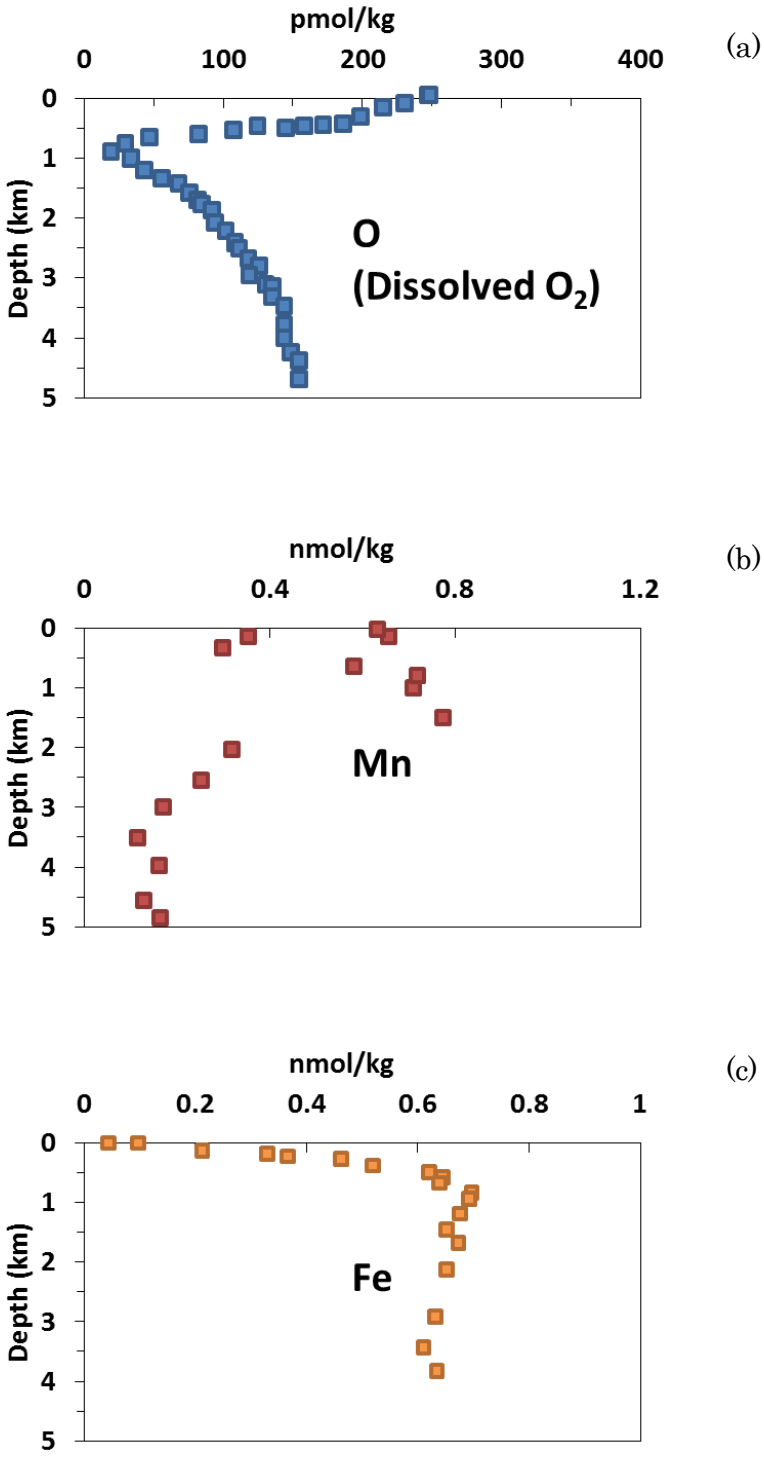

Figure I-1 Vertical concentration profiles of dissolved oxygen (a), manganese (b) and iron (c) in the North Pacific. Modified from Nozaki (1992).

I-1-3 Formation process of marine ferromanganese nodule and crust

According to the idea of Daymond et al. (1984), the formation process of ferromanganese nodule and crust is divided into three categories: (1) hydrogenous origin, (2) diagenetic origin, and (3) hydrothermal origin, as shown in Fig. I-2.

The hydrogenous origin is the simplest process and marine ferromanganese nodule and crust are formed on the seamount by sedimentation of fine particles of Fe(III) and Mn(IV) hydrous oxides. When the particles pass through the oxygen minimum zone, although Fe(III) hydrous oxide is not reduced, Mn(IV) dioxide is reduced to Mn(II) to dissolve. The dissolved Mn(II) is oxidized again by abundant dissolved oxygen in deep layer flow in ocean and Mn(IV) oxide is precipitated. Fine particles of the Mn(IV) oxide sink to the seabed and marine ferromanganese nodule is formed. The major mineral of manganese dioxide formed by the process of hydrogenous origin is vernadite (δ-MnO_2) (Calvert and Price, 1977).

The diagenetic origin is the secondary process of formation and growth of marine ferromanganese nodule after dissolution of the primary Mn(IV) oxide particle in anoxic sediment with low dissolved oxygen concentration under seabed. In the process, only Mn(IV) oxide particle is reduced to dissolve and Fe(III) oxide particle does not dissolve. Accordingly, manganese can be separated from Fe(III) oxide particle. When the dissolved Mn(II) moves to the upper seabed and encounters with seawater with high dissolved oxygen concentration, the secondary ferromanganese nodule with higher Mn/Fe atomic ratio is precipitated compared with that of the primary ferromanganese nodule. The formation condition of diagenetic process is divided into two categories: oxic and suboxic conditions depending on redox potential (dissolved oxygen concentration). The mineral of Mn(IV) oxide formed by the diagenetic origin is buserite (Siegel and Tuner, 1983).

The hydrothermal origin is the deposition process by mixing of reducing

hydrothermal fluid containing abundant Mn(II) and Fe(II) and oxidizing seawater with high concentration of dissolved oxygen near seabed. As Fe(II) deposits as sulfide near the spout hole of hydrothermal fluid, ferromanganese nodule with high Mn/Fe atomic ratio is precipitated. Main mineral of the Mn(IV) oxide is todorokite (Usui et al., 1989). Most of marine ferromanganese nodule and crust are considered to be both hydrogeneous and diagenetic origins and widely distributed on seabed in ocean. The hydrothermal origin is independent of the hydrogenous and diagenetic origins. The ferromanganese nodule of hydrothermal origin is formed only in the hydrothermal area.

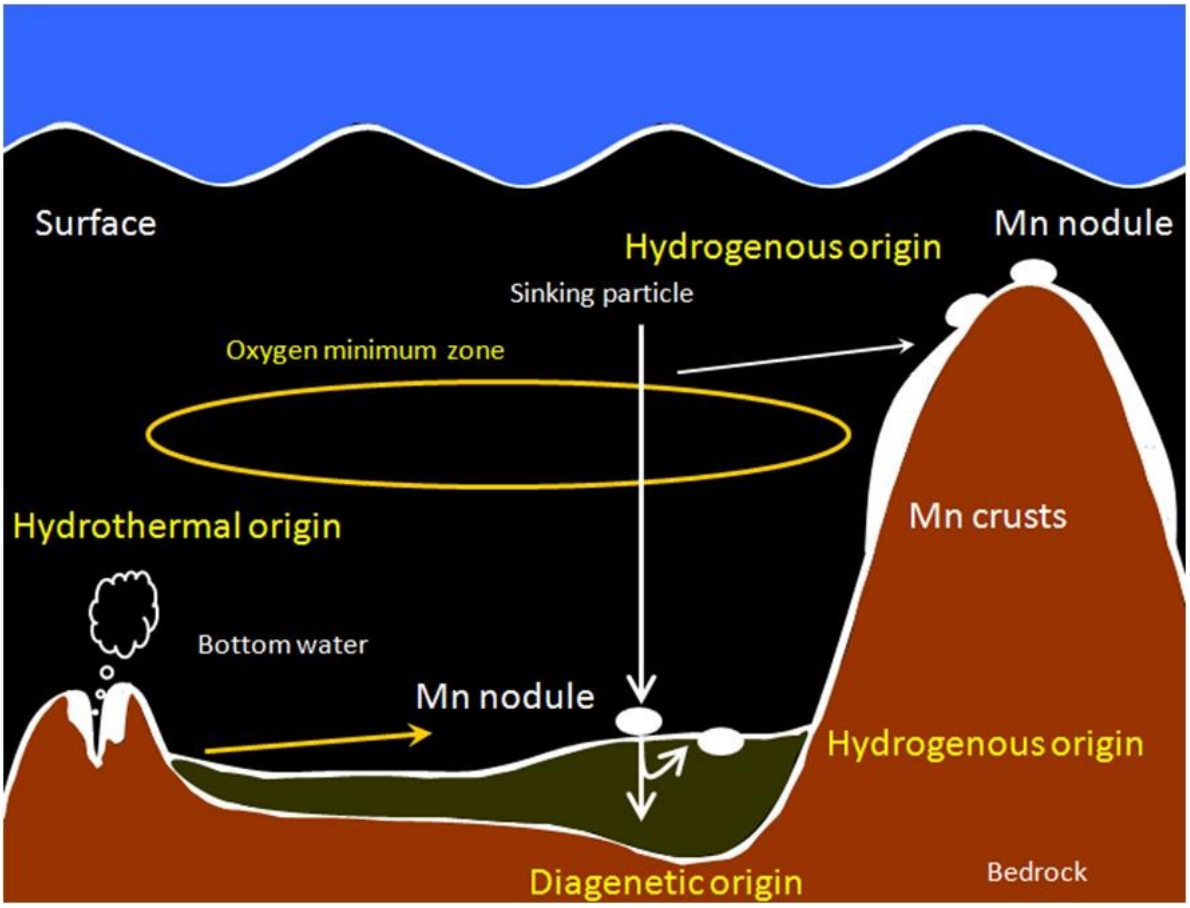

Figure I-2 Generation environment of ferromanganese nodule and crust in ocean. Blue: Atmosphere, Black: Ocean water, Brown: Base rock, Deep green: Sediment at seabed, White: Ferromanganese nodule and crust.

I-1-4 Uptake model of trace elements by marine ferromanganese nodule and crust

Figure I-3 shows a representative model for the uptake of trace elements by marine ferromanganese nodule and crust (Koschinsky and Halbach, 1995). Marine ferromanganese nodule and crust consist of mixture of Fe(III) oxide and Mn(IV) oxide. In seawater of pH 8, FeOOH particle, which is a representative hydrous ferric oxide, has positive charges on its surface, on the other hand, MnO_2 particle has negative charges. According to the electrostatic model in Fig. I-3, cations such as Ni(II) and Cu(II) are electrostatically sorbed on the surface of MnO_2, while carbonate complex anion of heavy rare earth elements and oxoanion such as MoO_4^{2-} are sorbed on hydrous ferric oxide.

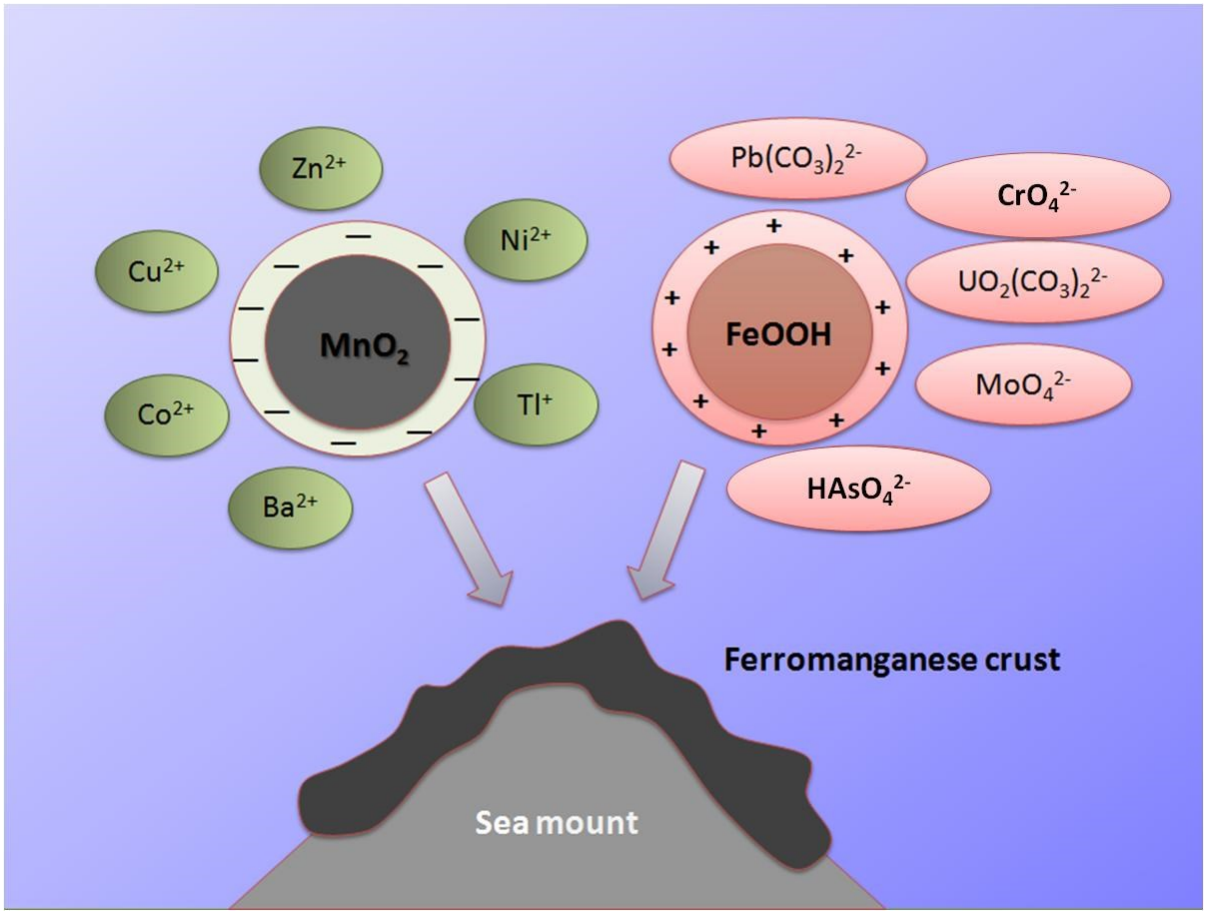

Figure I-3 A simplified electrochemical model for sorption of dissolved metal species on Fe(III) and Mn(IV) oxide phases in seawater, which are precipitated as a pavement on the flanks and summit of seamounts. Formation of colloidal or particulate Mn and Fe oxides is followed by sorption of oppositely charge ions on the charged surfaces of the oxide phases. Modified from Koschinsky and Halbach (1995).

I-1-5 Oxidative concentration mechanism of cobalt by marine ferromanganese nodule and crust - Validity of geochemical model experiment

It is well known that cobalt is highly concentrated into ferromanganese crust, which is hydrogeneous origin and is formed near the top of seamount. Since cobalt is essential in military industry, the concentration mechanism into ferromanganese crust has been vigorously investigated. As cobalt is present as divalent cation in seawater, it is electrostatically sorbed on MnO_2 particle with negative charges. First the uptake model of Co(II) onto MnO_2 particle was proposed by Burns (1976). In the model, Co(II) is incorporated into tunnel structure built up by octahedral MnO_6 units and then is oxidized to Co(III) as shown as eq.(I-1).

$$2Co^{2+}\ (\text{in solution}) + 2OH^- + 2H_2O + \delta\text{-}MnO_2\ (\text{solid}) \rightarrow$$
$$2Co(OH)_3\ (\text{in } \delta\text{-}MnO_2) + Mn^{2+}\ \ (\text{in solution}) \qquad (I\text{-}1)$$

The change in Gibbs free energy under the standard condition (ΔG^o) for the above reaction is -17.1 kcal mol^{-1}. The change in the ΔG^o of the eq.(1) indicates that oxidation of Co(II) to Co(III) by δ-MnO_2 occurs spontaneously. Figure I-4 shows the valence state, the electron configuration including high spin or low spin states and the corresponding ionic radius for cobalt and manganese ions. In the Fig. I-4, it should be remarkable that the ionic radius of Co(III) that has low spin state is close to that of Mn(IV). It suggests that the Co(III) may be substituted with Mn(IV), which is called isomorphous substitution. If the coordination structure and valence state of the corresponding chemical species are similar, the isomorphous substitution often occurs in nature. Consequently, Burns proposed that the oxidized cobalt may be substituted to Mn(IV) in octahedral MnO_6 units of δ-MnO_2 structure.

In order to confirm the idea, Burns (1976) and Murray et al. (1979) conducted

sorption experiments of Co(II) on manganese oxide and measured the valence state of cobalt ion sorbed by XPS. The result showed that the sorbed Co(II) is oxidized to Co(III).

Dillard et al. (1984) directly measured the valence state of cobalt in marine ferromanganese nodule by XPS and observed a peak at 780.3 eV which can be assigned to Co(III) ($Co2p_{3/2}$). In addition, the energy position for CoOOH (780.3 eV) is closer than that for Co_2O_3 (779.2 eV), suggesting that cobalt may be present as hydroxide rather than oxide in marine ferromanganese nodule (Buckley and Berg, 1986). This result demonstrates that when the content of target chemical species in marine ferromanganese nodule and crust is extremely low, the geochemical model reaction is often valid to elucidate the uptake behavior and the chemical state, although the concentration of the target chemical species in solution is higher than that in ocean.

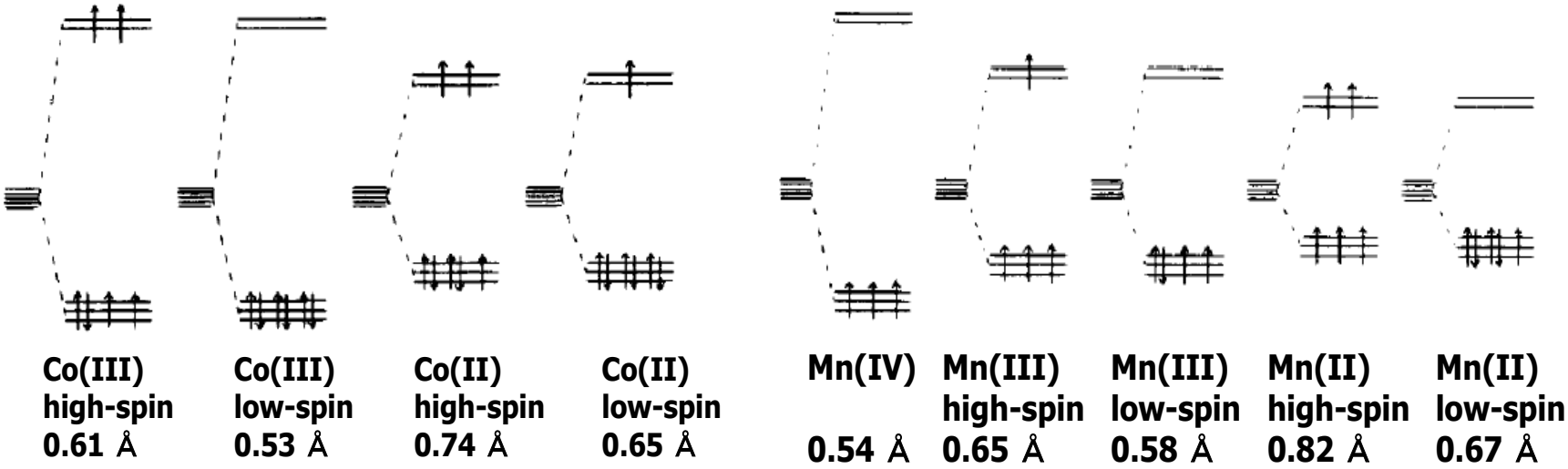

Figure I-4 Electronic configuration and ionic radius of Co and Mn ions (Burns, 1976).

I-2 Purpose of thesis

For the uptake of trace element in ocean by marine ferromanganese nodule and crust, the uptake of cerium (Ce) was also vigorously investigated in addition with that of cobalt (Elderfield et al., 1981; Calvert and Price, 1977). Since cobalt and cerium are rich in marine ferromanganese nodule and crust, their chemical state can be directly investigated by spectroscopic method such as XPS and XAFS. Based on the spectroscopic results, their uptake behavior can be also studied.

In the circulation of elements in hydrosphere, the elements dissolved into river water by the chemical weathering of rocks are incorporated into marine ferromanganese nodule and crust through ocean. Therefore, the content of trace elements in marine ferromanganese nodule and crust is often compared to that in earth crust. However, if certain element is concentrated into marine ferromanganese nodule and crust compared with that in seawater or in earth crust, its chemical state is not necessarily detected by the spectroscopic methods because of extremely low content. In this case, the geochemical model experiment is useful to elucidate the chemical state and the uptake behavior as described above.

There is no detailed information on the behavior of gold (Au) and platinum (Pt) concerning marine ferromanganese nodule and crust. Although several researchers studied on the uptake mechanism of Pt into marine ferromanganese nodule and crust, the problem has never been solved even at present. Whether Pt is sorbed as Pt(IV) (oxidative uptake) or Pt(0) (reductive uptake) has been in controversy since 1980. Even now, the chemical state of Au and Pt in marine ferromanganese nodule and crust has never been detected because of the low contents. As a result, no uptake behavior for Au and Pt by marine ferromanganese nodule and crust has also been investigated.

From the background for geochemistry of Au and Pt concerning marine ferromanganese nodule and crust described above, I tried to investigate the uptake

mechanism of Au and Pt by the geochemical model reaction in this thesis. As Au and Pt are present as complex anion such as $[AuCl_{4-n}(OH)_n]^-$ and $[PtCl_{4-n}(OH)_n]^{2-}$ ($1 \leqq n < 4$) in seawater, the sorption behavior onto δ-MnO_2 was investigated under various conditions and the chemical states of Au and Pt sorbed onto δ-MnO_2 was examined by XPS and XAFS for Pt and ^{197}Au Mössbauer spectroscopy for Au.

If the uptake mechanism of various elements by marine ferromanganese nodule and crust shown in Fig. I-3 is correct, Au and Pt should be sorbed on hydrous ferric oxide phase and cannot be sorbed on hydrous manganese(IV) oxide phase due to electrostatic repulsion. However, there is a linear relationship between the contens of Mn and Pt in marine ferromanganese nodule and crust, on the other hand, there is an inverse relationship between the contents Fe and Pt (Terashima et al., 1989). Ohashi et al. (2005) reported that $[AuCl_{4-n}(OH)_n]^-$ complex anion is rapidly sorbed on δ-MnO_2. The facts suggest that the uptake of Au and Pt by marine ferromanganese nodule and crust may be controlled by other reactions than electrostatic reaction which overcome the electrostatic repulsion between negative surface charges on δ-MnO_2 (PZC is around pH 4) and negative charge of the complex anions. The purpose of this thesis is to elucidate the uptake mechanism of Au and Pt by marine ferromanganese nodule and crust based on the suitable geochemical model reactions.

References

Buckley P. J. M. and van den Berg C.M.G. (1986) Copper complexation profiles in the Atlantic ocean. A comparative study using electrochemical and ion exchange techniques. *Mar. Chem.* **19**: 281-296.

Burns R. G. (1976) The uptake of cobalt into ferromanganese nodules. soils. and synthetic manganese (IV) oxides. *Geochim. Cosmochim. Acta* **40**: 95-102.

Calvert S. E. and Price N. B. (1977) Geochemical variation in ferromanganese nodule and associated sediment from the Pacific Ocean. *Mar.Chem.* **5**: 43-74.

Daymond J., Lyle M., Finny B., Piper D. Z., Murphy K., Conard R. and Pisias N. (1984) Ferromanganese nodule from MANOP sites H, S, and R - Control of mineralogical and chemical composition by multiple accretionary processes. *Geochim.Cosmochim.Acta* **48**: 931-949.

Dillard J. G., Crowther D. L. and Calvert S. E. (1984) X-ray photoelectron spectroscopic study of ferromanganese nodule: Chemical speciation for selected transition metals. *Geochim. Cosmochim. Acta* **48**: 1565-1569.

Elderfield H., Hawkesworth C. J. and Greaves M. J. (1981) Rare-earth element geochemistry of oceanic ferromanganese nodules and associated sediments. *Geochim. Cosmochim. Acta* **45**: 513-528.

Koschinsky A. and Halbach P. (1995) Sequential leaching of marine ferromanganese precipitates: Genetic implications. *Geochim. Cosmochim. Acta* **59**: 5113–5132.

Murray J. W. and Dillard J. G. (1979) The oxidation of cobalt(II) adsorbed on manganese dioxide. *Geochim. Cosmochim. Acta* **43**: 781-787.

Nozaki Y. (1992) Trace elements in sea water: Their mean concentrations and North Pacific profiles. *Chikyukagaku (Geochemistry)* **26**: 25-39.

Ohashi H., Ezoe H., Okaue Y., Kobayashi Y., Matsuo S., Kurisaki T., Miyazaki A., Wakita H. and Yokoyama T. (2005) The Effect of UV Irradiation on the Reduction of Au(III) Ions Adsorbed on Manganese Dioxide. *Anal. Sci.*, **21** : 789-793.

Siegel M. D. and Turner S. (1983) Crystalline todorokite associated with biogenic debris in manganese nodules. *Science* **219**: 172-174.

Terashima S., Usui A., Nakao S. and Mita N. (1989) Geochemistry of platinum and gold in ocean-floor ferromanganese crusts and nodules. *Bull. Geol. Surv. Japan* **40**: 127-141.

Usui A., Mellin T., Nohara M. and Yuasa M. (1989) Structure stability of marine 10 Å manganese from the Ogasawara (Bonin) Arc: Implications for low-temperature activity. *Mar.Geol.* **86**: 1-56.

Chapter II
Sorption mechanism of Pt(II) complex anion on Manganese dioxide and their spontaneous oxidation to Pt(IV)

II-1 Introduction

When considering the transport of trace elements in the hydrosphere, it is important to investigate the geochemical uptake mechanisms on the surfaces of various solids. The ferromanganese crust and nodule are among the representative solids in the ocean. It is well established that transition metals such as cobalt, copper, zinc and nickel are concentrated in marine ferromanganese nodule. However, only a few reports have been published for platinum in marine ferromanganese crust and nodule, despite the fact that Pt is an element with a much higher concentration in the ferromanganese crust than in the Earth's continental crust through ocean (Takematsu, 1998; Usui, 2010). The mechanism by which Pt is concentrated into marine ferromanganese crust has attracted attention for its potential applications in "Energy innovation such as fuel cell" in the future or even at present because of the demand of much Pt as an electrode and a catalyst.

According to studies by some researchers, Pt is enriched in ferromanganese crust and nodule collected from the Pacific Ocean: the Pt content varies from 6 ppb to 940 ppb (Agiorgitis and Gundlach,1978; Halbach, 1984; Hodge et al., 1985). Halbach et al. also reported the Pt content in ferromanganese crusts from the Central Pacific seamount areas ranges from 0.14 to 1.02 ppm (Halbach et al., 1989). The average Pt content was 0.51±0.24 ppm, indicating that ferromanganese crust and nodule contain more than 100 times the concentration of Pt compared to the Pt concentration of ~5 ppb in the Earth's upper continental crust (Halbach, 1984). According to Terashima et al., there was a moderate positive correlation between Mn and Pt contents in samples from both the Ogasawara Plateau ($r = 0.55$) and the Antarctic Ocean ($r = 0.66$), while no clear

correlation between Fe and Pt was observed (Terashima et al., 1989). In the Ogasawara Plateau and the Central Pacific seamount, Fe and Pt were negatively correlated ($r = -0.57$). These observations suggest that Pt in the manganese dioxide phase can be found in ferromanganese crusts that are a mixture of hydrous iron(III) oxide and manganese dioxide (δ-MnO_2). The Pt concentration in ocean water increases from 0.1 ppt in shallow water (~200 m) to 0.3 ppt in deep water (>2000 m) (Halbach et al., 1989). Relative to the Pt concentration in ocean, the ferromanganese crusts contain on average more than 2×10^6 times as much Pt. The dominant species of dissolved Pt in ocean water are considered to be Pt(II) complex ions from a thermodynamic consideration (Halbach et al., 1989). Although it is necessary to investigate the chemical state of Pt in ferromanganese crust to elucidate the uptake and concentration mechanisms, no investigation has been published because of the extremely low Pt content. We cannot directly observe the chemical state of Pt in ferromanganese crust by spectroscopic methods.

Because Pt is difficult to study directly, the sorption of Pt(II) complex anions onto δ-MnO_2 may provide a suitable model reaction for elucidating the uptake and concentration mechanisms of Pt from ocean water into ferromanganese crust. Therefore, in this investigation, the sorption behavior of Pt(II) complex anions on the surface of δ-MnO_2 was examined. Moreover, Pt species sorbed on δ-MnO_2 were characterized by XPS and XAFS. This investigation describes chemical reactions at the geochemical interface between solid minerals and water, which is one of the most important reaction spaces for understanding the behavior of trace elements in the hydrosphere.

II-2 Experimental

II-2-1 Reagents and sample solutions

All reagents used were of analytical grade (Wako Pure Chemical Industry). All the solutions were prepared with pure water (Milli-Q SP system, Millipore). K_2PtCl_6 or K_2PtCl_4 was dissolved with water to prepare the stock solution (1000 ppm and 5000 ppm as Pt). The Pt solutions for the sorption experiments were prepared by diluting the stock solutions. The Pt concentration of the solutions was determined by Inductively coupled plasma emission spectrometry (ICP-ES). Manganese dioxide (CMD 200, specific surface area: 203 $m^2\ g^{-1}$) as an sorbent of Pt(II) and Pt(IV) complex ions was supplied from Chuo Denki Kogyo Co., Ltd. The manganese dioxide was δ-MnO_2 that is X-ray amorphous.

II-2-2 Procedures

The sorption experiments were conducted at room temperature by a batch method. All the sorption experiments were conducted in a dark room to avoid the effects of light. The pH of the Pt solution (5 - 500 ppm Pt) with NaCl (0.12 mol dm^{-3}) as a supporting electrolyte was adjusted to the desired pH by dropping NaOH solution, and the appropriate amount of δ-MnO_2 powder was added. The pH was continuously monitored using a glass electrode equipped with a pH meter. The pH was maintained within ± 0.1. The suspended solution was magnetically stirred (stirring rate: 300 rpm). At adequate intervals, aliquots of the suspension were taken out and filtered with a 0.45 μm membrane filter (cellulose acetate) for collection of filtrate and with 0.40 μm membrane filter (glass fiber) for collection of the solid sample to prevent the reduction of the Pt(II) complex ion that was sorbed on the δ-MnO_2 by cellulose acetate. The Pt concentration in the filtrate was determined by ICP-ES. The solid samples remained on the filter were

dried in a vacuum desiccator at ambient temperature under dark conditions. The proportion of Pt sorbed was estimated according to equation (II-1):

$$\text{Sorption proportion (\%)} = [(C_0 - C) / C_0] \times 100 \qquad \text{(II-1)}$$

Here, C_0 indicates the initial Pt concentration in solution and C indicates the concentration in solution at t (reaction time).

II-2-3 XPS measurement

The chemical state of Pt in solid samples was analyzed by XPS (Shimadzu KRATOS - AXIS 165). Powder sample adhered to the carbon tape was placed in an evacuated sample chamber (under 10^{-10} torr, and at room temperature). The XPS spectra were acquired using a monochromatic Al Kα X-ray source (1486.49 eV) operated at 30 W (15 keV, 2 mA). Survey spectra were collected over the range 0 - 1400 eV with pass energy of 80 eV. High resolution XPS spectra were acquired for C1s, O1s, Mn2p, and Pt4f using pass energy equal to 40 eV. In all cases, the photoelectron take-off angle was 45°. The XPS spectra were corrected internally using the peak position of Cls as a standard (284.6 eV) because the sample charging can shift the peak position in the XPS spectra. The spectra were obtained under conditions of 0.1 eV steps and the acquisition of 298 ms/point. The binding energies of Pt(II), Pt(IV) and Pt(0) states were obtained from K_2PtCl_4, K_2PtCl_6 and Pt wire as standard materials of Pt(II), Pt(IV), and Pt(0), respectively. The Shirley method was used to correct the background. After the corrections, the spectra were analyzed using a *XPS PEAK 4.1* computer software.

II-2-4 XAFS measurement

The chemical states of Pt in solid samples were also analyzed by X-ray absorption fine structure (XAFS). Pt L_3-edge XAFS measurements were carried out at BL37XU of SPring-8 (Hyogo, Japan). The storage ring energy was 8 GeV with a typical current of 99.5 mA. Pt L_3-edge (11.56 keV) XAFS spectra were measured using a Si(111) double crystal monochromator. XAFS data of the samples for Pt L_3-edge were collected under ambient conditions in fluorescence mode. A 19 – element Ge solid – state detector (19SSD) was used to measure the intensity of the incident X-rays. XAFS data of the standard materials (K_2PtCl_4, K_2PtCl_6, $K_2Pt(OH)_6$ and Pt foil as Pt(II), Pt(IV), Pt(IV) and Pt(0)) at the Pt L_3-edge were collected under ambient conditions. The spectral analysis was carried out by the XAFS analytical softwares, Athena and Artemis (Ravel and Newville, 2005). The extraction of the extended X-ray absorption fine structure (EXAFS) oscillation from the spectra, normalization by edge-jump, and Fourier transform were performed by Athena. The curve-fitting analysis was carried out in R-space by Artemis. k-range was 3.0 – 10.2 $Å^{-1}$ and r-range was 1.9 – 3.4 Å. In the curve-fitting analysis, the backscattering amplitude, phase shift, and the mean-free path of the photoelectron were calculated by FEFF8.4 (Ankudinov et al., 1998), and then the other parameters, that is, the number of neighboring atoms, the inter atomic distance between the absorbed atom to the neighboring atom, the Debye-Waller factor, and the absorption edge energy were treated as fitting parameters. The intrinsic loss factor was obtained by the curve-fitting analysis of the EXAFS data of the $K_2Pt(OH)_6$ (Pt(IV)).

II-2-5 TEM observation

TEM images of the solid samples were obtained by Philips CM 20 transmitted electron microscope.

II-2-6 Zeta Potential

In order to examine the surface charge of δ-MnO_2, its zeta potential in NaCl solution (0.12 mol dm^{-3}) was measured in the pH range 2-7 using a Malvern Zeta Master.

II-2-7 Chloride ion selective electrode

In order to confirm the hydrolysis of $PtCl_4^{2-}$ ion (substitution of Cl^- with H_2O or OH^- ion), solid K_2PtCl_4 was dissolved in water. The variation of Cl^- ion concentration with time was measured using the Cl^- ion selective electrode (DKK-TOA CL-125B) equipped to a ion meter (DKK-TOA ION MATER IM-40S). In the titration experiment, the amount of OH^- ion added to maintain the initial pH of 8 was compared to the amount of Cl^- ion released in the solution. pH was measured at the same time using a pH meter (HORIBA pH MATER F-22).

II-3 Results and Discussion

II-3-1 Sorption behavior of Pt(II) and Pt(IV) complex ions

Figure II-1 shows the variation in the proportion of sorption for Pt(II) and Pt(IV) complex ions on δ-MnO_2 with time for 6 h at pH 8. The initial concentration of Pt was 5 ppm, and 5 or 10 g of δ-MnO_2 was added. This initial Pt concentration was selected for the sensitivity of ICP-ES. Approximately 40 ~ 50 % of Pt(II) complex ion was sorbed on δ-MnO_2 after 6 h, but no Pt(IV) complex ion could be sorbed even after 6 h.

Figure II-2 shows the proportion of Pt(II) complex ions sorbed on δ-MnO_2 at various pH after 24 h. The proportion was highest at pH 6. However, the Pt(II) complex ion can be effectively sorbed on δ-MnO_2 even in the pH range of 8 – 10. This finding indicates that the Pt(II) complex ion can be significantly sorbed on δ-MnO_2 from ocean water, which has a pH of approximate 8. However, no Pt(IV) complex ion could be sorbed in the pH range 2 - 10. We examined the hydrolysis of the $[PtCl_4]^{2-}$ complex ion (the substitution of Cl^- with OH^- for the $[PtCl_4]^{2-}$ complex ion) at pH 8 to identify the Pt(II) species that would preferentially sorb onto δ-MnO_2. Because Li et al., Jeanette et al., and Azaroual et al. reported that Cl^- ion in $[PtCl_4]^{2-}$ complex ion can substitute with H_2O molecule (Li et al., 1990; Jeanette et al., 2002; Azaroual et al., 2001), and $[AuCl_4]^-$ hydrolyzes to $[AuCl_{4-n}(OH)_n]^-$ even at weak acid condition depending on Cl^- concentration.

When solid of K_2PtCl_4 is dissolved into water, whether Cl^- ion in the $[PtCl_4]^{2-}$ complex ion is substituted with H_2O molecule or OH^- ion has been uncertain even at present. In a preliminary experiment in this study, it was confirmed that when K_2PtCl_4 was dissolved into water, Cl^- ion was released and pH of the solution decreased. Therefore, immediately after K_2PtCl_4 was dissolved into water of pH8 (pH was adjusted to 8 by adding the small amount of NaOH solution before the titration experiment), the titration of NaOH standard solution was started. To maintain pH to 8, the titration was

conducted. Figure II-3 shows the variation of amount of Cl^- ion released into water with time and the amount of OH^- ion added to maintain pH to 8. The Cl^- concentration increased with decreasing OH^- concentration (pH) in the solution, suggesting that Cl^- ion in $[PtCl_4]^{2-}$ complex can be substituted with OH^- ion in water. Figure II-3 suggests that the hydroxyl group is key to the sorption of Pt(II) complex ions on δ-MnO_2. Since the PZC (point of zero charge) of δ-MnO_2 is approximately pH 4 and hydrolytic species ($[PtCl_{4-n}(OH)_n]^{2-}$, n = 1 ~ 4) form at pH 8, they can specifically sorb on δ-MnO_2 to form a Mn-O-Pt bond by a condensation reaction between the surface OH^- group on δ-MnO_2 and the OH^- group in the Pt(II) complex ion. Surprisingly, this condensation reaction is a strong reaction that overcomes the electrostatic repulsion between the negatively charged surface of δ-MnO_2 above pH 4 and the Pt(II) complex anion.

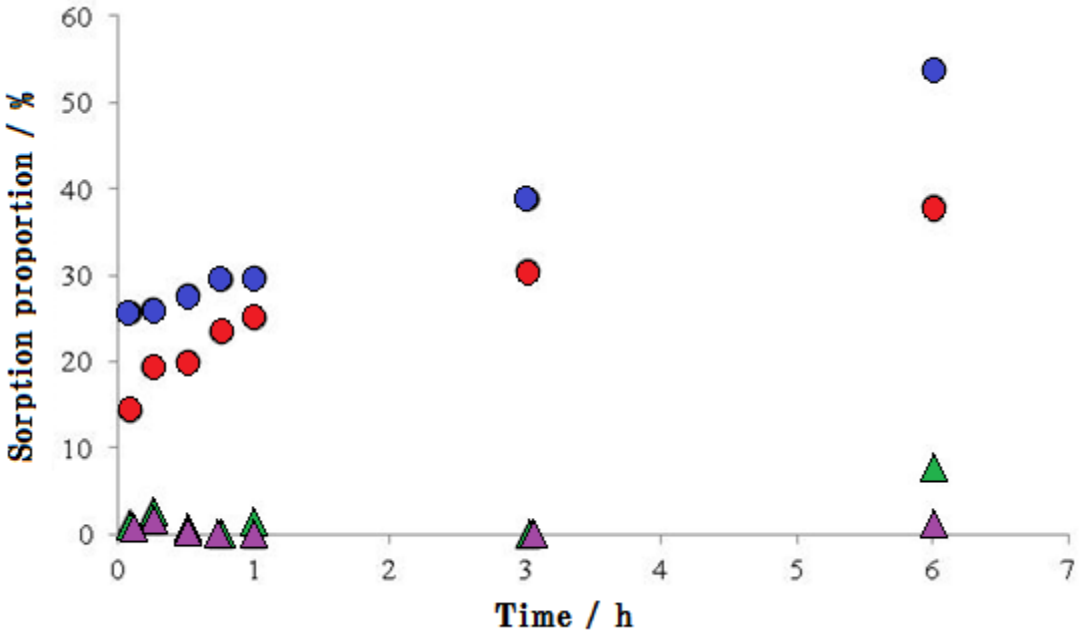

Figure II-1 Variation of sorption proportion for Pt(II) complex ions (●, ●) and Pt(IV) complex ions (▲, ▲) on δ-MnO_2 with time. Initial Pt concentration: 5 ppm. The amount of δ-MnO_2 added: 10 g (●, ▲) and 5 g (●, ▲). pH: 8. Volume: 0.5 dm^3. NaCl concentration: 0.12 mol dm^{-3}.

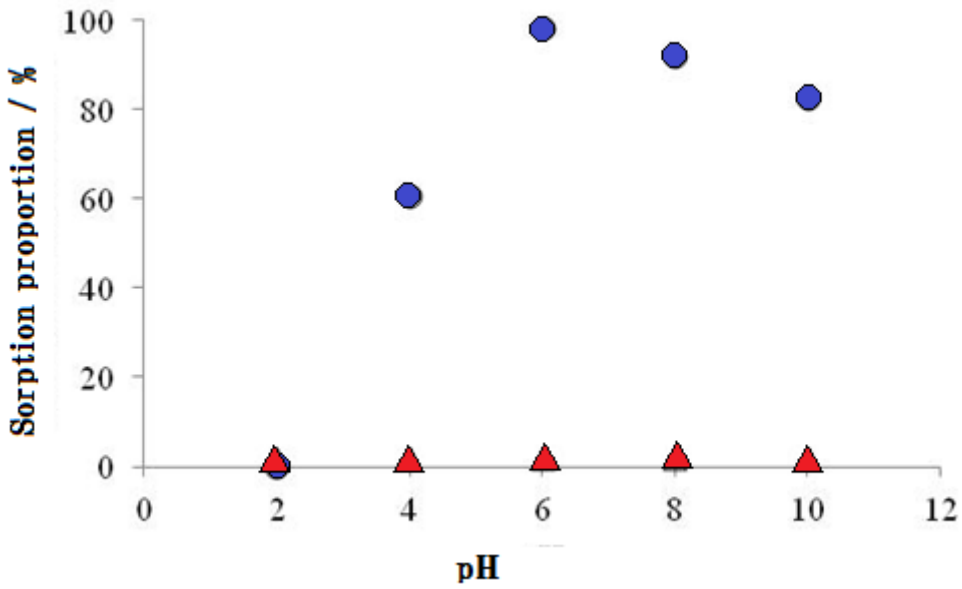

Figure II-2 Sorption proportion of Pt(II) complex ions (●) and Pt(IV) complex ions (▲) on δ-MnO_2 at various pHs. Initial Pt concentration: 5 ppm. The amount of δ-MnO_2 added: 5 g. Volume: 0.5 dm^3. Reaction time: 24 h.

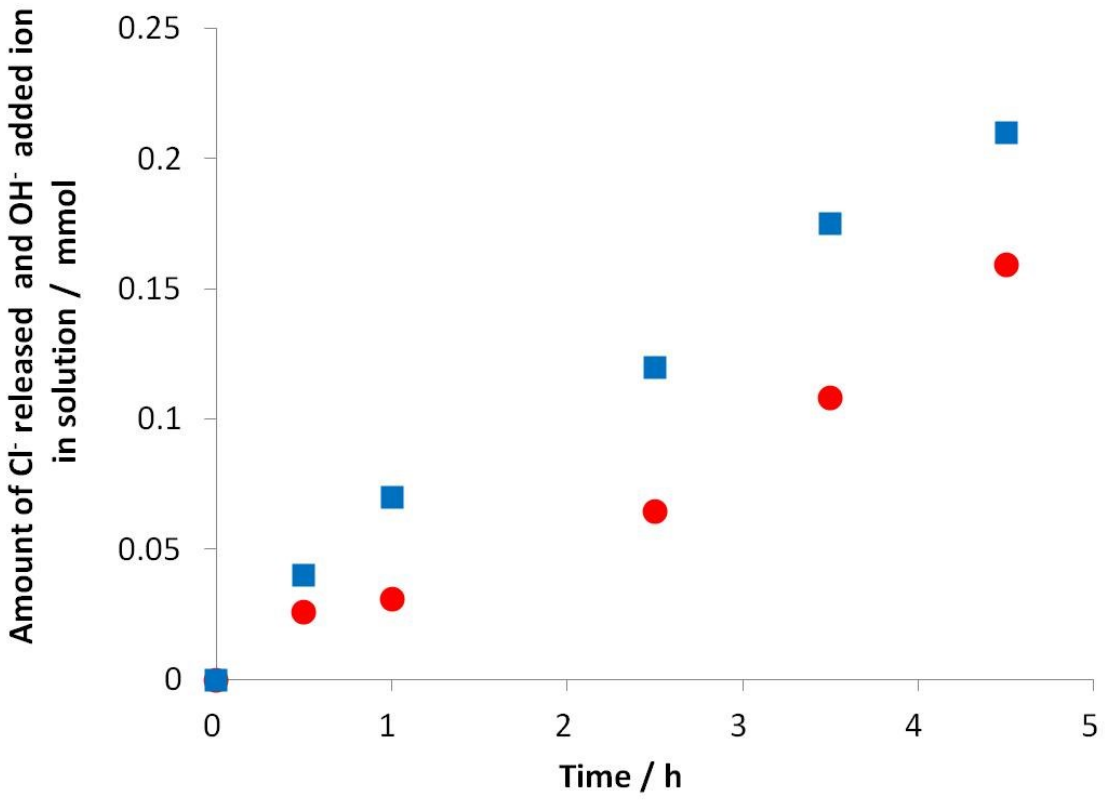

Figure II-3 A relationship between the amount of Cl^- (●) released from $[PtCl_4]^{2-}$ complex ion sorbed and the amount of OH^- (■) added. The standard NaOH solution was titrated into solution to maintain the pH to 8. A 53 mg of K_2PtCl_4 (solid) was dissolved into water (0.5 dm^3) of pH 8.

II-3-2 Oxidation state of Pt sorbed on δ-MnO_2

Halbach et al. and Terashima et al. proposed that Pt may be present as Pt(0) in ferromanganese crusts that are formed at depths with minimum dissolved oxygen concentrations as shown in Figs 1 and 2 (Halbach et al., 1989; Terashima et al., 1989). In contrast, some researchers have proposed oxidative sorption of Pt(II) to Pt(IV) on ferromanganese crusts (Hodge et al., 1985; Halbach et al., 1989; Goldberg et al., 1987; Banakar et al., 2007). Whether the Pt(II) complex ion is taken up as Pt(0) or Pt(IV) by ferromanganese crusts remains uncertain even at present. Ohashi et al. have found that when the Au(III) complex ion is sorbed on δ-MnO_2, the Au(III) is reduced to Au(0) (Ohashi et al., 2005a; Ohashi et al., 2005b). Therefore, to examine whether Pt(0) particles were present on δ-MnO_2, the solid sample (δ-MnO_2 sorbing Pt) was first observed by TEM. In spite of the careful TEM observation, no Pt(0) particles were found in TEM images.

Next, to examine the valence state of Pt sorbed on δ-MnO_2, the XPS spectra for solid samples were measured. When preparing solid samples for XPS measurement in this sorption experiment, the initial Pt concentration was set at 500 ppm because of the low sensitivity of XPS. Figure II-4(a) shows Pt4f XPS spectra for standard materials as Pt(0), Pt(II) and Pt(IV). From the XPS spectra, Pt(0), Pt(II) and Pt(IV) can be distinguished. Figure II-4(b) shows the Pt4f spectra of a solid sample (δ-MnO_2 sorbing Pt). It shows two doublet peaks. The peaks were assigned to Pt(II) and Pt(IV) by comparing the peak position to those of the standard materials. The major component of Pt sorbed on δ-MnO_2 is Pt(IV), and Pt(II) is a minor component. However, Pt(IV) could not sorb on δ-MnO_2, as shown in Figs. II-1 and II-2. After sorption of Pt(II), Pt was fixed tightly, despite the fact that Pt(II) was oxidized to Pt(IV).

II-3-3 Dissolution of Mn during sorption of the Pt(II) complex ion on δ-MnO_2

The XPS data described here confirms that the Pt(II) complex ion is oxidized to Pt(IV) after sorption on δ-MnO_2. The oxidation/reduction potential for the conversion from Pt(II) to Pt(IV) and from Mn(IV) to Mn(II) can be represented as follows although the oxidation reaction potential of hydrolytic species for Pt(II) and Pt(IV) is uncertain.

$$PtCl_6^{2-} + 2e^- \rightleftarrows PtCl_4^{2-} + 2Cl^- \qquad E_0 = +0.68\ V \qquad (II\text{-}2)$$

$$MnO_2 + 4H^+ + 2e^- \rightleftarrows Mn^{2+} + 2H_2O \qquad E_0 = +1.2\ V \qquad (II\text{-}3)$$

Based on equations (II-2) and (II-3), although the Pt complex species sorbed on δ-MnO_2 may be different from the $[PtCl_4]^{2-}$ complex ion, the oxidant of the sorbed Pt(II) is expected to be Mn(IV) in δ-MnO_2. If this is correct, one Mn(II) should be released into solution after the oxidation of one Pt(II) to Pt(IV) by Mn(IV) because of transfer of two electrons from Pt(II) to Mn(IV). Therefore, the variation of Mn and Pt concentrations with time were simultaneously measured during the sorption experiment. The sorption experiment was performed at pH 4 to avoid the re-sorption/precipitation of the released Mn(II) on δ-MnO_2. In fact no release of Mn was observed at pH 8. As shown in Fig. II-5, although the amount of Mn(II) released into solution was less than the amount of Pt sorbed, a considerable amount of the Mn was dissolved during the sorption of the Pt(II) complex ion. A part of the Mn that is dissolved into solution may be re-sorbed on δ-MnO_2. The data indicate that after sorption of Pt(II) on δ-MnO_2, the Pt(II) is oxidized by Mn(IV) in δ-MnO_2 through a Mn-O-Pt(II) bond.

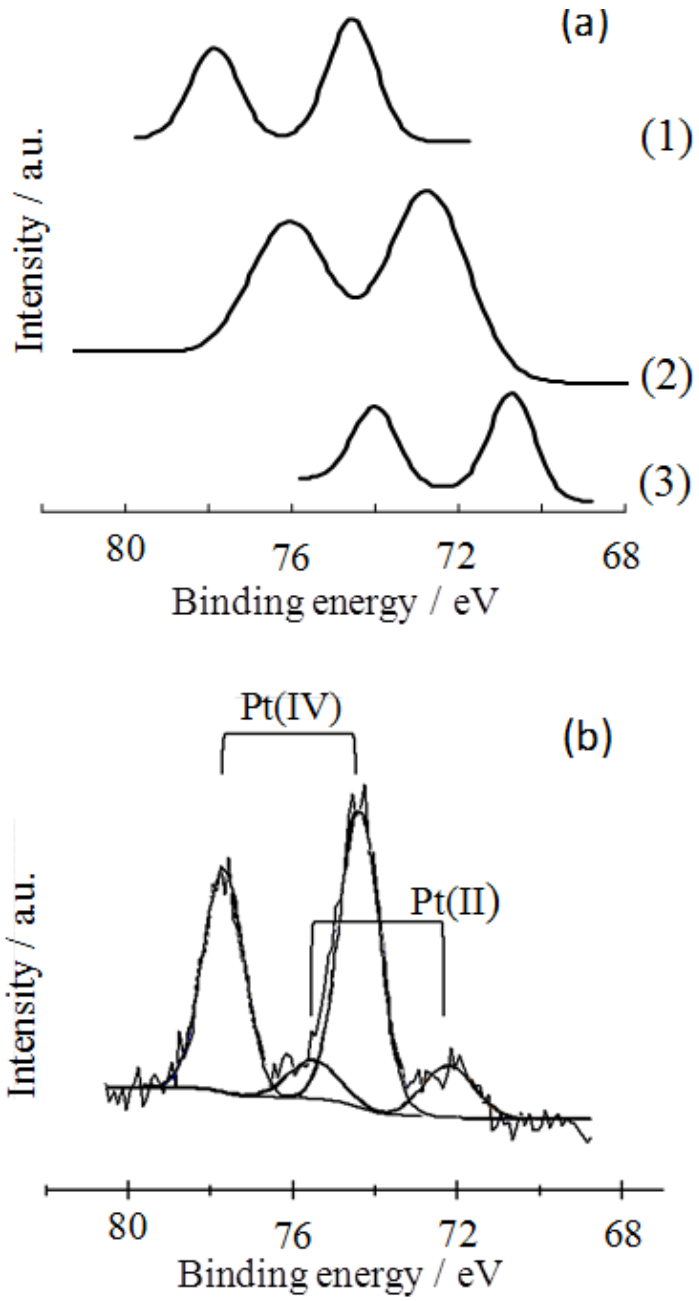

Figure II-4 Pt4f XPS spectra of standard materials (a) and a solid sample (b). Standard materials: K_2PtCl_6 (1), K_2PtCl_4 (2), Pt wire (3). Doublet peak positions of Pt4f spectra for standard materials were 74.6 and 77.9 eV (Pt(IV)), 72.7 and 76.0 eV (Pt(II)), and 70.7 and 74.0 eV (Pt(0)). Initial Pt concentration: 500 ppm. The amount of δ-MnO_2 added: 10 g. pH: 8. Volume: 0.5 dm^3. NaCl concentration: 0.12 mol dm^{-3}. Reaction time: 24 h. The fitted peak positions for the solid sample were 72.2 and 75.5 eV (Pt(II)) and 74.4 and 77.7 eV (Pt(IV)).

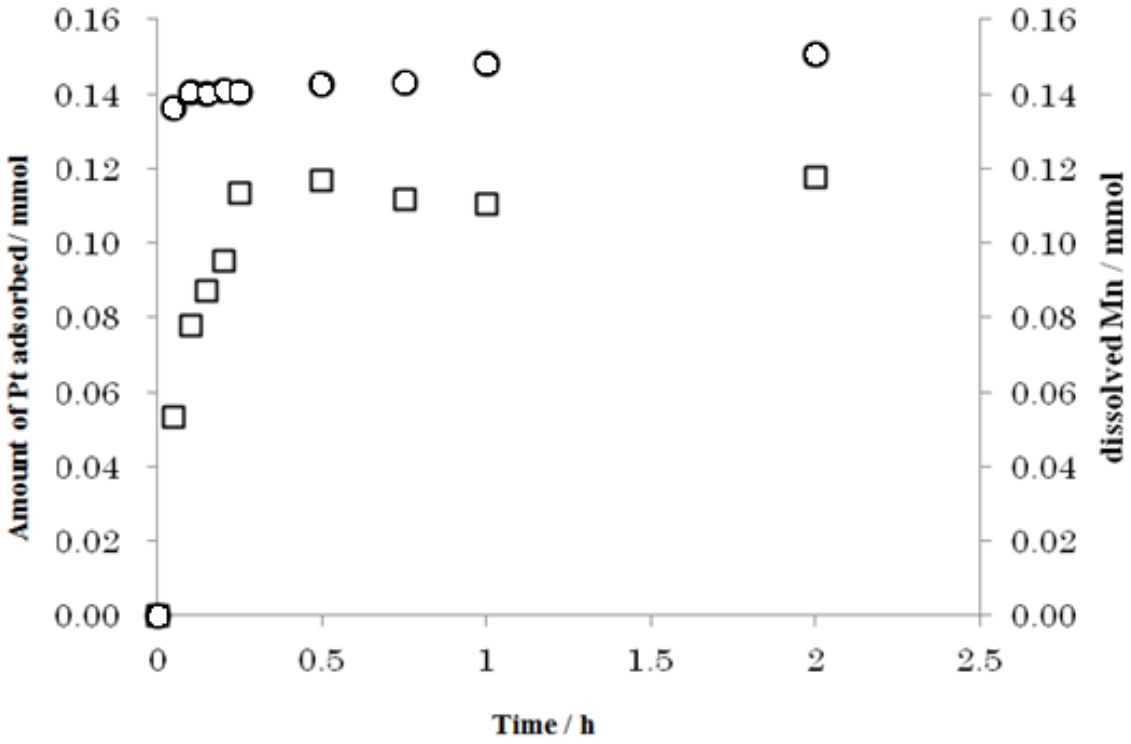

Figure II-5 Variations in the amount of sorbed Pt (○) on δ-MnO_2 and the amount of dissolved Mn(□) with time. Initial Pt concentration: 100 ppm. Amount of δ-MnO_2 added: 5 g. pH: 4. Volume: 0.5 dm^3. NaCl concentration: 0.12 mol dm^{-3}.

II-3-4 Structure of Pt sorbed on δ-MnO_2

To examine the structure of Pt sorbed on δ-MnO_2, XAFS measurement was conducted. Figure II-6 shows Pt L_3 - edge XANES spectra for standard materials of Pt (a – e) and the Pt sorbed on δ-MnO_2 with various contents (f – i) (solid samples). The position of first peaks for Pt(0) and Pt(II) was different from that for Pt(IV) and solid samples. The shape of spectra of the solid samples is clearly different from that of Pt wire. The facts indicate that Pt sorbed on δ-MnO_2 is not Pt(0) but Pt(IV). Moreover, although the spectra of K_2PtCl_4 and K_2PtCl_6, which chloride ions coordinate to Pt ion, have a distinctive peak (＊ in Figure II-6) around 11.57 – 11.58 keV, the spectra of $Pt(acac)_2$ and $K_2Pt(OH)_6$, which oxide ions coordinate, do not show the peak. The solid samples did not show the peak around 11.57 – 11.58 keV and the shape of their spectra closely resembles that of $K_2Pt(OH)_6$. Judging from the results of XPS spectra in Fig. II-4 and XANES spectra in Fig. II-6, it can be reasonably concluded that Pt(II) sorbed on δ-MnO_2 is oxidized to Pt(IV) accompanying ligand exchange from chloride ion to hydroxide ion. In addition, it should be emphasized here that structure conversion from square planar 4-coordinate structure for Pt(II) to 6-coordinate octahedral structure for Pt(IV) occurred.
To determine the detailed coordination structure of Pt sorbed on δ-MnO_2, the EXAFS analysis was conducted. Based on the above interpretation of XPS and XANES spectra, two structure parameters were considered: (1) the valence state of Pt sorbed on δ-MnO_2 is Pt(IV) and (2) the coordination structure is PtO_6 system. In Fig. II-4, no Pt(0) component was observed and the amount of Pt(IV) was considerably larger than that of Pt(II). It can be easily deduced that if the amount of Pt sorbed on δ-MnO_2 is low, the existence of Pt(II) can be ignored. All of atoms coordinated to Pt(IV) are oxygen because no Cl^- was found in the wide XPS spectra, and the shape of XANES spectra was quite similar between the solid sample and $[Pt(OH)_6]^{2-}$ as a Pt(IV) standard material .

Figure II-7 shows the k^3-weighed EXAFS oscillation for the corresponding standard materials (a - e) and the solid samples (f - i) in Fig. II-6. One of the most important points is that all the spectra for the solid samples (f - i) closely resemble each other and the spectra are almost the same as that of spectrum for $K_2Pt(OH)_6$ as a standard material (e). These facts indicate that chemical state of Pt in the solid samples (f - i) is almost the same in spite of different amount of Pt sorbed on δ-MnO_2 and the valence state is Pt(IV). In addition, the phase of the spectra for the solid samples at k = 8.5 – 8.7 $Å^{-1}$ is opposite against that of K_2PtCl_4 and K_2PtCl_6 as standard materials (b and c). This opposite phase may be due to difference from coordinated atoms, that is, chlorine or oxygen. From this fact, it can be supposed that the atoms coordinated to Pt in the solid samples are oxygen and the coordination structure is PtO_6 system.

The radial structure functions which are Fourier transformations of the EXAFS oscillations are shown in Fig. II-8. The structural parameters CN (coordination number), R (inter atomic distance, Pt-O), and the σ^2 (Debye-Waller factor) were obtained by fitting the curve for the first shell EXAFS data in R space. The parameters obtained are summarized in Table II-1. These EXAFS functions fitted well, and the fitted EXAFS functions indicate that the interatomic distance for Pt-O in the solid sample was 1.99 Å and that the CN was 6. Consequently, interatomic distance for Pt-O in the solid sample coincides with that of $K_2Pt(OH)_6$.

II-3-5 Oxidative uptake model reaction of Pt by δ-MnO_2

Based on the above data, Fig. II-9 shows a schematic figure of the model reaction for the concentration of Pt onto marine ferromanganese crusts whose manganese phase consists of δ-MnO_2.

Pt(II) ($[PtCl_{4-n}(OH)_n]^{2-}$) can be sorbed on δ-MnO_2 and then the Pt(II) is oxidized to Pt(IV), to which six oxygen atoms coordinate. One of the reasonable interpretations for this sorption and oxidation/reduction mechanism of Pt(II) onto δ-MnO_2 is that there is an isomorphous substitution between Pt(IV) and Mn(IV) by oxidation of Pt(II) to Pt(IV) and reduction of Mn(IV) to Mn(II) through a Mn-O-Pt bond. The abundance of cobalt in ferromanganese crust is considered to be due to isomorphous substitution between Mn(III) and Co(III) as a result of the oxidation of Co(II) to Co(III) and the reduction of Mn(IV) to Mn(III) (Burns, 1976; Murray and Dillard, 1979). The release of Mn(II) from δ-MnO_2 during the sorption of Pt(II), as shown in Fig. II-5, proves that the proposed oxidative uptake of Pt(II) including the isomorphous substitution is reasonable.

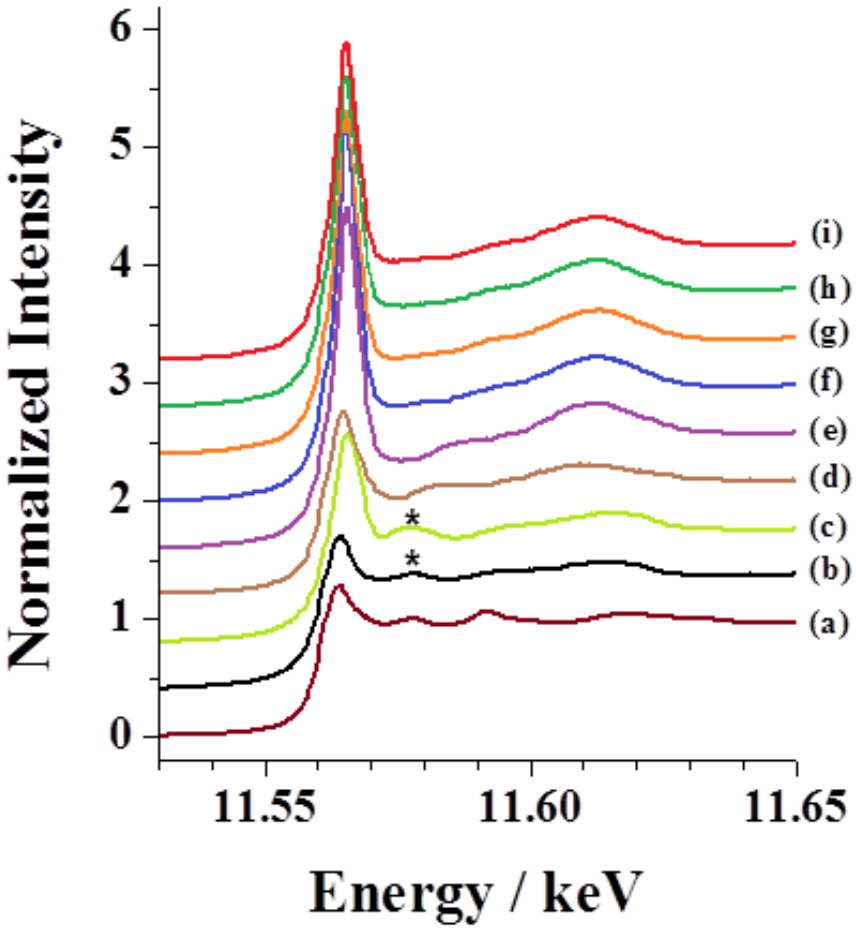

Figure II-6 Pt L_3-edge XANES spectra for standard materials of Pt(0), Pt(II) and Pt(IV) (a - e) and Pt species sorbed on δ-MnO_2 (f - i). Standard materials: Pt wire (a), K_2PtCl_4 (b), K_2PtCl_6 (c), $Pt(acac)_2$ (d), $K_2Pt(OH)_6$ (e). Initial Pt concentration and weight % of Pt: 500 ppm 2.5 wt% (f), 200 ppm 1.0 wt% (g), 100 ppm 0.5 wt% (h), 50 ppm 0.25wt% (i). The amount of δ-MnO_2 added: 10 g. pH: 8. Volume: 0.5 dm^3. NaCl concentration: 0.12 mol dm^{-3}. Reaction time: 24 h. Resolution of Pt L_3 XANES spectra: 0.0003 keV.

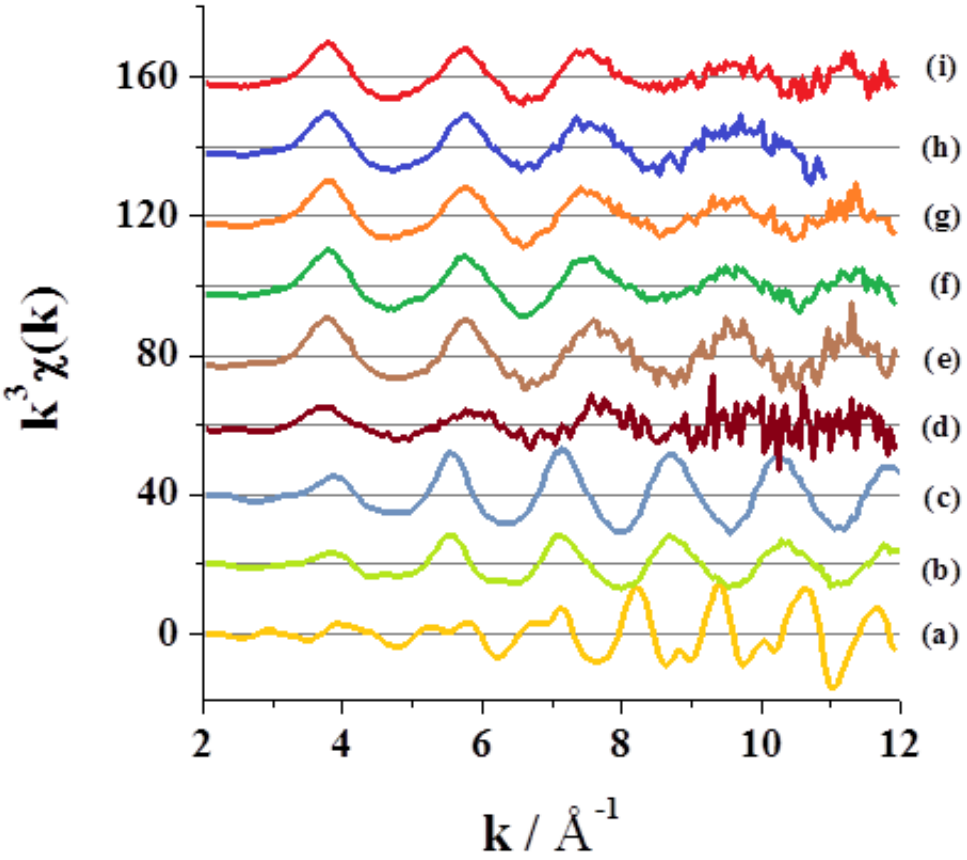

Figure II-7 The k^3-weighted EXAFS oscillations for standard materials (a - e) and solid samples (f - i) shown in Fig. II-6.

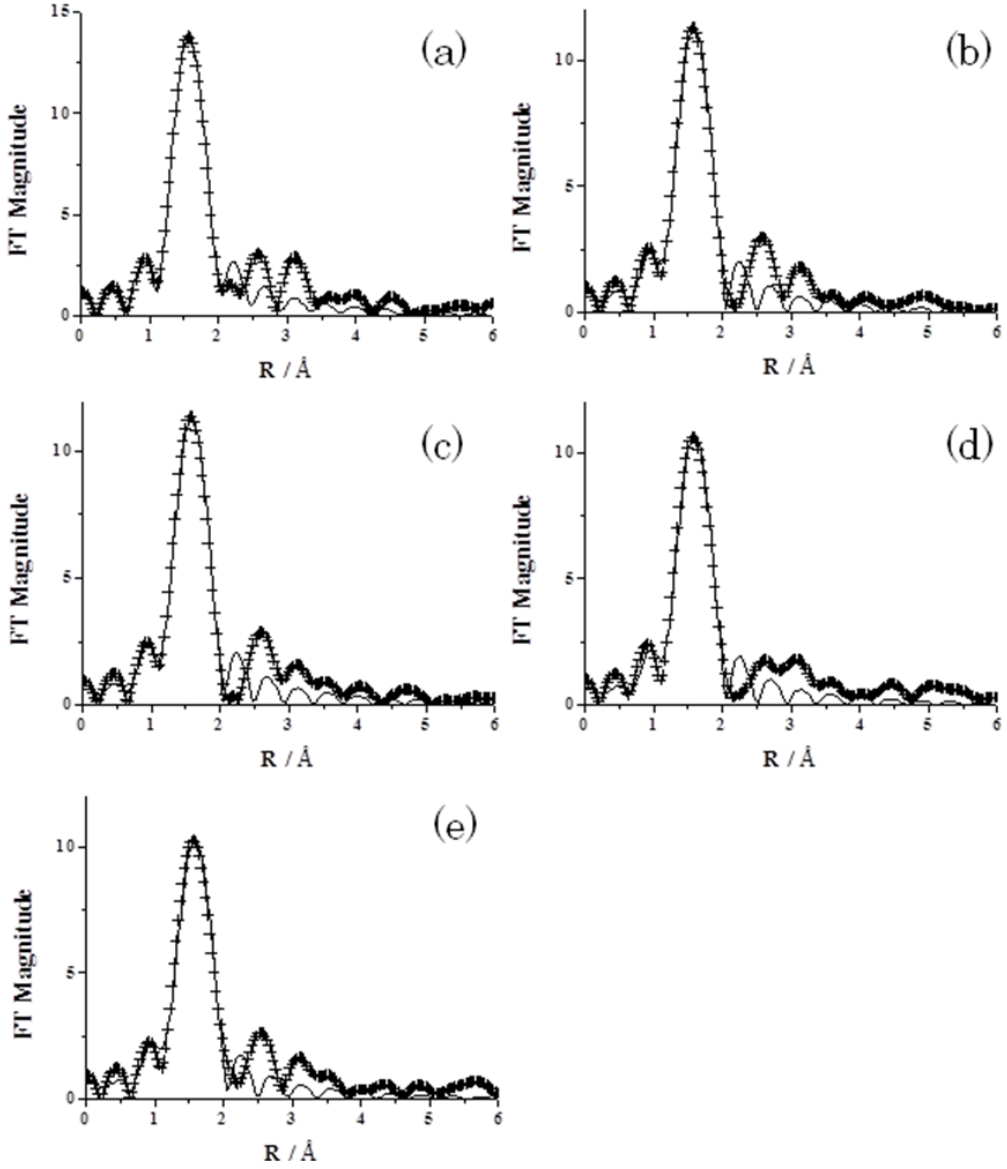

Figure II-8 Radial structure functions for (a) $K_2Pt(OH)_6$ as a standard material of Pt(IV) and solid samples : initial Pt concentration and weight % of Pt: 500 ppm 2.5 wt% (b), 250 ppm 1.0 wt% (c), 100 ppm 0.5 wt% (d), 50 ppm 0.25 wt% (e). (+ :Fourier transform data, －: Fitting line)

Table II-1 EXAFS fitting parameters of solid samples and standard materials.

sample	Shell	CN	R / Å	σ^2 / 10^{-3} Å^2	R_{factor} (%)
$K_2Pt(OH)_6$	Pt-O	6.0±0.5	2.00±0.01	0.9±0.7	0.071
Pt/MnO_2 (500ppm)	Pt-O	6.8±1.9	2.02±0.02	4.1±3.0	0.496
Pt/MnO_2 (200ppm)	Pt-O	6.5±1.2	2.02±0.01	3.7±1.9	0.255
Pt/MnO_2 (100ppm)	Pt-O	6.3±1.8	2.02±0.02	3.9±3.0	0.639
Pt/MnO_2 (50ppm)	Pt-O	6.9±2.6	2.02±0.02	5.4±4.2	1.056

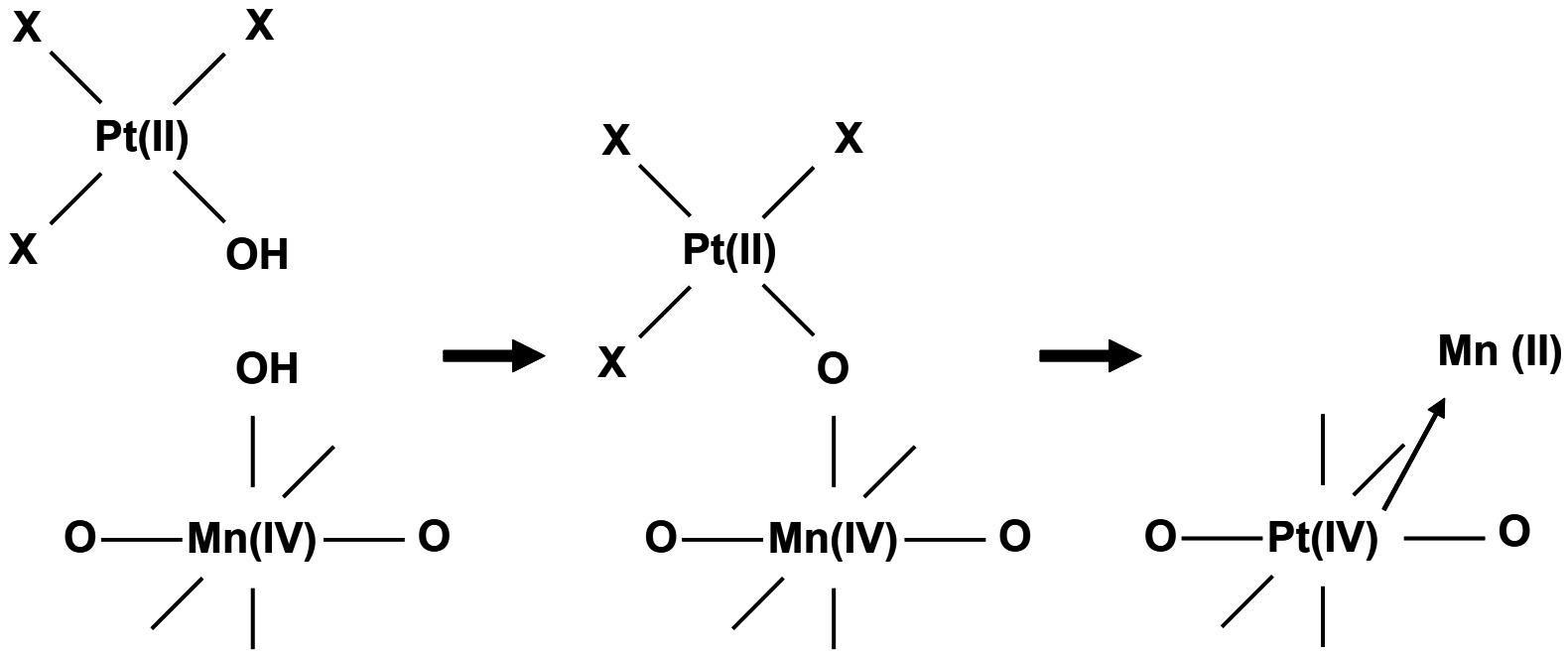

Figure II-9 A proposed model of concentration mechanism for Pt onto δ-MnO_2 through the isomorphous substitution between Pt(IV) and Mn(IV) ions. X = Cl^-, OH^-.

References

Agiorgitis G. and Gundlach H., (1978) Platin-Gehalte in Tiefsee-Manganknollen. *Naturwissenschaften* **65**: 534.

Ankudinov A. L., Ravel B., Rehr J. J. and Conradson S. D. (1998) Real-space multiple-scattering calculation and interpretation of x-ray-absorption near-edge structure *Phys. Rev. B* **58**: 7565-7576.

Azaroual M., Romand B., Freyssinet P. and Jean R. D. (2001) Solubility of platinum in aqueous solutions at 25℃ and pHs 4 to 10 under oxidizing conditions. *Geochim. Cosmochim. Acta* **65**: 4453-4466.

Banakar V. K., Hein J. R., Rajani R. P. and Chodankar A. R. (2007) Platinum group elements and gold in ferromanganese crusts from Afanasiy-Nikitin seamount, equatorial Indian Ocean: Sources and fractionation. *J.Earth Syst. Sci.* **116**: 3-13.

Burns R. G. (1976) The uptake of cobalt into ferromanganese nodules. soils. and synthetic manganese (IV) oxides. *Geochim. Cosmochim. Acta* **40**: 95-102.

Goldberg E D, Hodge V, Kay P, Stallard M and Koide M (1986) Some comparative marine chemistries of platinum and iridium. *Appl. Geochem.* **1** : 227-232.

Halbach P. (1984) Deep-sea metallic deposits. *Ocean Management* **9**: 35-60.

Halbach P., Kriete C., Prause B. and Puteanus D. (1989) Mechanisms to explain the platinum concentration in ferromanganese seamount crusts. *Chem. Geol.* **76**: 95-106.

Hodge V. F., Stallard M., Koide M. and Goldberg E. D. (1985) Platinum and the platinum anomaly in the marine environment. *Earth Planet. Sci. Lett.* **72**: 158-162.

Jeanette M. C. and Byrne R. H. (2003) Comparative geochemistries of Pd(II) and Pt(II): Formation of mixed hydroxychloro and chlorocarbonate-complexes in seawater. *Geochim. Cosmochim. Acta.* **67**: 1331-1338.

Li W., Brigitte E., Schwederski and Dale W. M. (1990) Stepwise Hydrolysis Kinetics of Tetrachloroplatinate (II) in Base. *Inorg. Chem.* **29**: 3578-3584.

Murray J. W. and Dillard J. G. (1979) The oxidation of cobalt(II) sorbed on manganese dioxide. *Geochim. Cosmochim. Acta* **43**: 781-787.

Ohashi H., Ezoe H., Yamashige H., Okaue Y., Matuo S., Kurisaki T., Wakita H. and Yokoyama T. (2005a) Reduction behavior of Au(III) complex ions adsorbed on the surface of manganese dioxide: XPS study. *Adv. X-Ray Chem. Anal. Jpn.* **36**: 339-345.

Ohashi H., Ezoe H., Okaue Y., Kobayashi Y., Matsuo S., Kurisaki T., Miyazaki A., Wakita H. and Yokoyama T. (2005b) The Effect of UV Irradiation on the Reduction of Au(III) Ions Adsorbed on Manganese Dioxide. *Anal. Sci.*, **21** : 789-793.

Takematsu N. (1998) Manganese nodule -Its formation mechanism and role. *Kouseishakouseikaku Co., Ltd., Japan.*

Terashima S., Usui A., Nakao S. and Mita N. (1989) Geochemistry of platinum and gold in ocean-floor ferromanganese crusts and nodules. *Bull. Geol. Surv. Japan* **40**: 127-141.

Ravel B. and Newville M. (2005) ATHENA, ARTEMIS, HEPHAESTUS: data analysis for X-ray absorption spectroscopy using IFEFFIT. *J. Synchrotron Radiat.* **12** : 537-541.

Usui A. (2010) "Mineral resources of the seabed". *Ohmsha*.

Chapter III
Simultaneus sorption of Pt(II) and Au(III) complex anions on manganese dioxide (δ-MnO_2) and their coupled redox behavior

III-1 Introduction

Although the amount is in trace level, precious metals such as gold (Au) and platinum (Pt) are contained in various rocks. They are transported into ocean by river water after chemical weathering of the rocks. Through circulation of these metals in ocean, they are sorbed and concentrated into marine manganese crust. At present it is well known that Pt is the second element that is concentrated into marine manganese crust through seawater compared with the content in earth crust (Takematsu, 1998; Usui, 2010). Due to the extremely high concentration factor of Pt, the uptake mechanism into marine manganese crust has been vigorously investigated by some researchers. Pt is considered to be present as Pt(II) in seawater from the thermodynamic condition (Halbach et al., 1989). Whether the Pt(II) is sorbed as Pt(IV) or Pt(0) has been discussed for long time (Hodge et al., 1985; Halbach, 1984; Halbach, 1986; Halbach et al., 1989). We cannot detect directly and spectroscopically the chemical state of Pt in marine manganese crust because of extremely low concentration. However, I solved the scientific problem from geochemical model reactions with higher concentration than actual concentration of Pt in marine manganese crust. The model reaction was the sorption of Pt(II) complex anion into δ-MnO_2 and the chemical state of Pt sorbed into δ-MnO_2 was measured by XPS and XAFS. The δ-MnO_2 is considered to be host mineral of Pt in marine manganese crust (Terashima et al., 1989). From the results of the XPS and XANES spectra, the Pt(II) is oxidized to Pt(IV) by Mn(IV) in MnO_2. From the analytical result of the EXAFS spectra for Pt, the Pt(IV) is substituted with Mn(IV) , which is released as Mn(II), after the sorption (Chapter II in this thesis). On the other

hand, until the end of the 20th century, only a few analytical data for gold (Au) in marine manganese crust have been published. As the reported Au content of marine manganese crust was not high, the geochemical study on gold in marine manganese crust had scarcely been carried out. If Au is present as Au(III) in seawater, it has the same 4-coordinate square planar structure as that of Au(III) ($[PtL_4]^{2-}$ and $[AuL_4]^-$, L = Cl^- or OH^-). Therefore, some geochemists referred to a geochemical mystery why the Au content is lower than that of Pt in marine manganese crust (Koide et al., 1986).

According to the recently compiled analytical data of major and minor elements in marine manganese crust (Hein et al., 2013), however, Au is also concentrated into marine manganese crust through seawater compared with the content of Au in earth crust. Therefore, we carried out the statistical analysis for contents of Au and Pt in marine manganese crusts using data of Hein et al. Figure III-1 shows the analytical result (sample numbers = 93 (Au) and 147 (Pt)). The horizontal axis and vertical axis indicate the concentration values of Pt and Au in marine manganese crusts, respectively. These concentration values are normalized by the concentration values of Pt and Au in seawater because of cancellation of the effect of difference in concentration against their sorption into marine manganese crust. In the normalization the concentration values of Pt and Au in seawater reported by Nozaki (Nozaki, 1992) were used. As shown in Fig. III-1, there is a good linear relationship between the contents of Pt and Au in marine manganese crust. The correlation coefficient is 0.84. This result suggests that the sorption mechanism of Pt and Au into marine manganese crust may be coupled. As described above, Pt(II) is sorbed into δ-MnO_2 by the oxidative substitution. In contrast with the sorption behavior of Pt, a part of Au(III) sorbed into δ-MnO_2 is spontaneously reduced to elemental gold (Au(0)) (Ohashi et al., 2005). These facts indicate high affinity of Pt and Au to δ-MnO_2.

The each sorption mechanisms of Pt and Au into δ-MnO_2 are evidently different. However, the two different sorption mechanisms were proposed from single sorption experiments of Pt(II) or Au(III) complex anion into δ-MnO_2. The purpose of this study is to elucidate reason for the correlation between the contents of Pt and Au in marine manganese crust by competitive sorption experiments into δ-MnO_2 in the presence of both Pt(II) and Au(III) complex anions. Although the Pt and Au concentrations in solutions used in this study were extremely high compared with those in seawater, the minimal Pt and Au concentrations were selected to detect the chemical states of Pt and Au by XPS, XAFS, and ^{197}Au Mössbauer spectroscopy.

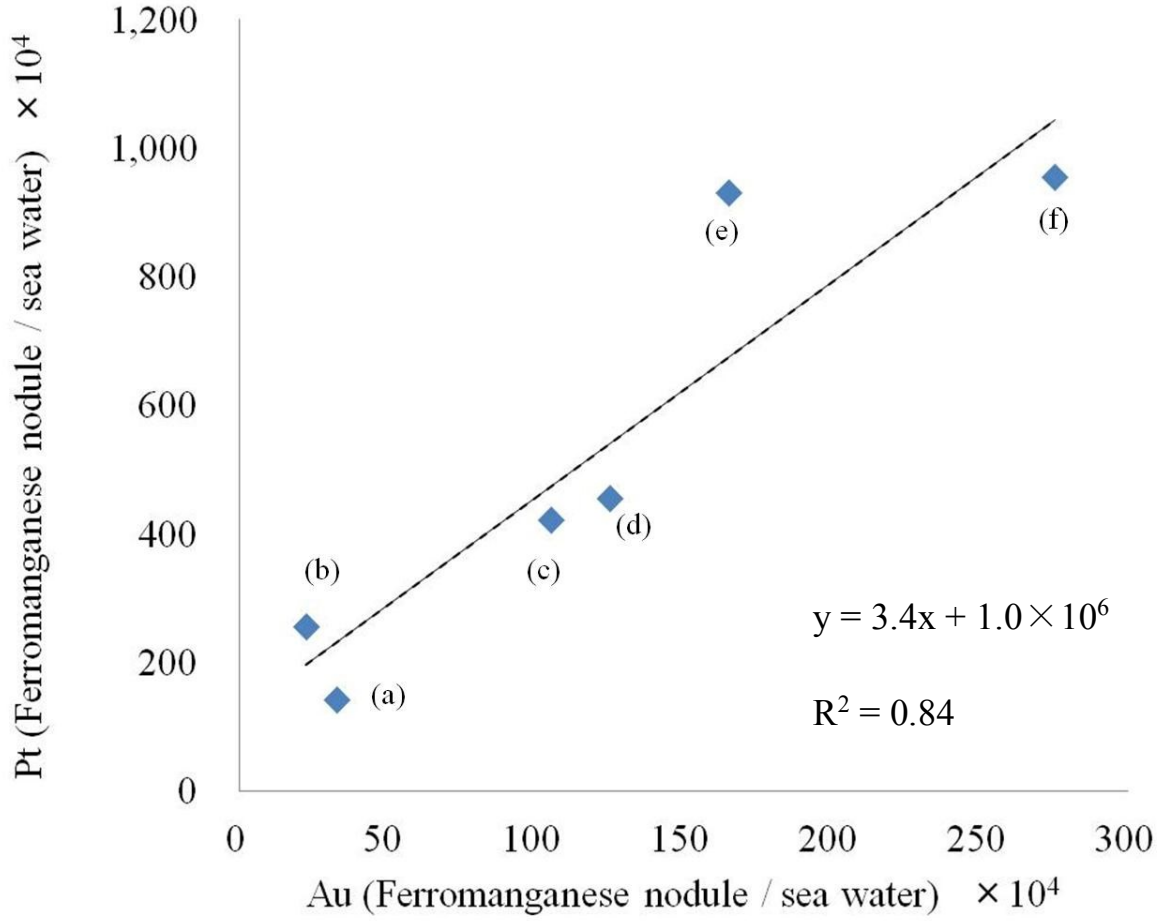

Figure III-1 A relationship between the contents of Pt and Au in marine manganese crusts. This figure was built up based on the analytical data by Hein et al. (2013). The contents of Pt and Au in marine manganese crusts are normalized by the concentrations of Pt and Au in seawaters which were reported by Nozaki (1992). One plot shows the mean value of Pt and Au contents in marine manganese crusts collected in the same region. (a) CA margin, N_{Au}=10, N_{Pt}=23 (b) CCZ nodules, N_{Au}=9, N_{Pt}=13 (c)Indian Ocean, N_{Au}=2, N_{Pt}=6 (d) Non-Prime N. Pacific, N_{Au}=21, N_{Pt}=24 (e) S. Pacific, N_{Au}=38, N_{Pt}=15 (f) N. Pacific Prime Zone, N_{Au}=13, N_{Pt}=66.

III-2 Experimental

III-2-1 Reagents and sample solutions

All reagents used were of analytical grade (Wako Pure Chemical Industry). All the solutions were prepared with pure water (Milli-Q SP system, Millipore). K_2PtCl_4 or $HAuCl_4 \cdot 4H_2O$ was dissolved with water to prepare stock solution (5,000 ppm). The mixed sample solutions containing both Au and Pt for the sorption experiments were prepared by diluting the stock solutions. The Pt and Au concentrations of the solutions were determined by Inductively Coupled Plasma Emission Spectrometry (ICP-ES). Manganese dioxide (δ-MnO_2, CMD 200, specific surface area: 203 $m^2\ g^{-1}$) as an sorbent of Pt(II) and Au(III) complex ions was supplied from Chuo Denki Kogyo Co., Ltd. The manganese dioxide was δ-MnO_2 that is X-ray amorphous.

III-2-2 Procedure

The sorption experiments were conducted at room temperature using a batch method. All the sorption experiments were conducted in a dark room to avoid the effects of light. The pH of the Pt and Au mixed solution (5 - 100 ppm Pt or Au) with NaCl (0.12 mol dm^{-3}) as a supporting electrolyte was adjusted to the desired pH by dropping NaOH solution, and the appropriate amount of δ-MnO_2 powder was added. The pH was continuously monitored using a glass electrode equipped with a pH meter. The pH was maintained within ± 0.1. The suspended solution was magnetically stirred (stirring rate: 300 rpm). At adequate intervals, aliquots of the suspension were taken out and filtered with a 0.45 μm membrane filter (cellulose acetate) for collection of filtrate and with 0.40 μm membrane filter (glass fiber) for collection of the solid sample to prevent the reduction of the Pt(II) complex ion that was sorbed onto the δ-MnO_2 by cellulose acetate. The Pt concentration in the filtrate was determined by ICP-ES. The solid samples remained on

the filter were dried in a vacuum desiccator at ambient temperature under dark conditions. The proportion of Pt and Au sorbed was estimated according to a following equation (III-1):

$$\text{Sorption proportion (\%)} = [(C_0 - C) / C_0] \times 100 \qquad \text{(III-1)}$$

Here, C_0 indicates the initial Pt or Au concentration in solution and C indicates the concentration in solution at a reaction time t.

III-2-3 Measurement of ^{197}Au Mössbauer spectra

The chemical state of Au in the solid samples was measured by ^{197}Au Mössbauer spectroscopy (homemade equipment). The ^{197}Pt isotope ($T_{1/2}$ = 18.3 h), γ -ray source feeding the 77-keV Mössbauer transition of ^{197}Au, was prepared by neutron irradiation of isotopically enriched ^{196}Pt metal at the Kyoto University Research Reactor. The absorbers were particle specimens. The source and specimens were cooled with a helium refrigerator. The temperature of the specimens was in the range 13–14 K. The zero-velocity point of the spectra was the peak point of pure bulk Au. The spectra of all solid samples were fitted with single Lorentzian lines.

III-2-4 Measurement of XAFS spectra

The chemical states of Pt in solid samples were also analyzed by X-ray absorption fine structure (XAFS). Pt L_3-edge XAFS measurements were carried out at BL14B2 of SPring-8 (Hyogo, Japan). The storage ring energy was 8 GeV with a typical current of 99.5 mA. Pt L_3-edge (11.56 keV) XAFS spectra were measured using an Si(311) double crystal monochromator. The XAFS data of the solid samples and standard materials (K_2PtCl_4, K_2PtCl_6, $K_2Pt(OH)_6$ and Pt foil as Pt(II), Pt(IV), Pt(IV) and Pt(0) were collected

under ambient conditions in transmission mode. Ionization chambers were used to measure the intensity of the incident X-rays. The spectral analysis was carried out by the XAFS analytical softwares, *Athena and Artemis* (Ravel and Newville, 2005).

III-3 Results and Discussion

III-3-1 Sorption affinity of Au(III) and Pt(II) complex anions onto δ-MnO_2

In order to compare the sorption affinity of Au(III) and Pt(II) complex anions to δ-MnO_2, the sorption experiments were carried out as shown in Figs. III-2 and III-3(a) and III-3(b). In the Fig. III-2 and Fig.III-3, the amount of δ-MnO_2 added was different (0.05 or 0.5 g). The reaction time was 6 h in all the experiments except that of Fig. III-2. In all the experiments except that of Fig. III-3(b), the amount of Au and Pt sorbed onto δ-MnO_2 approached to the limiting values within 24 h, however the amount of Au and Pt sorbed increased gradually even after several 10 h in the experiment shown in Fig. III-3(b).

Figure III-2 shows the variation of percent of Au sorbed onto δ-MnO_2 with time. The initial Au concentration was 50 ppm (as Au). The amount of δ-MnO_2 added was 0.05 g and the coexisting Pt concentrations were 0, 5, 10, and 15 ppm (as Pt). Surprisingly, the amount of Au sorbed increased with increasing the coexisting Pt concentration. The result indicates that Pt(II) complex anion may not prevent the Au sorption onto δ-MnO_2.

No sorption of Pt occurred under the above condition, suggesting that the sorption sites may be occupied by Au(III) complex ions. Perhaps, the amount of δ-MnO_2 added was too small compared with the amounts of Pt(II) and Au(III) complex anions in the solution.

Next, the another sorption experiment, which δ-MnO_2 of 0.5 g was added, was performed. Figure III-3(a) shows the variation of percent of Au sorbed with time. The initial Au concentration was 50 ppm and the coexisting Pt concentrations were 0, 10, 50, and 100 ppm. The sorption of Au was significantly accelerated with increase in the amount of δ-MnO_2 added. The sorption rate was also increased with increasing the coexisting Pt concentration, like the result shown in Fig. III-2. Figure III-3(b) shows the

variation of percent of Pt sorbed onto δ-MnO_2 with time. The initial Pt concentration was 50 ppm and the coexisting Au concentrations were 0, 5, 25, 50, and 100 ppm. The Pt sorption was confirmed to occur with increase in the amount of δ-MnO_2 added. However, the Pt sorption was retarded with increasing the coexisting Au concentration.

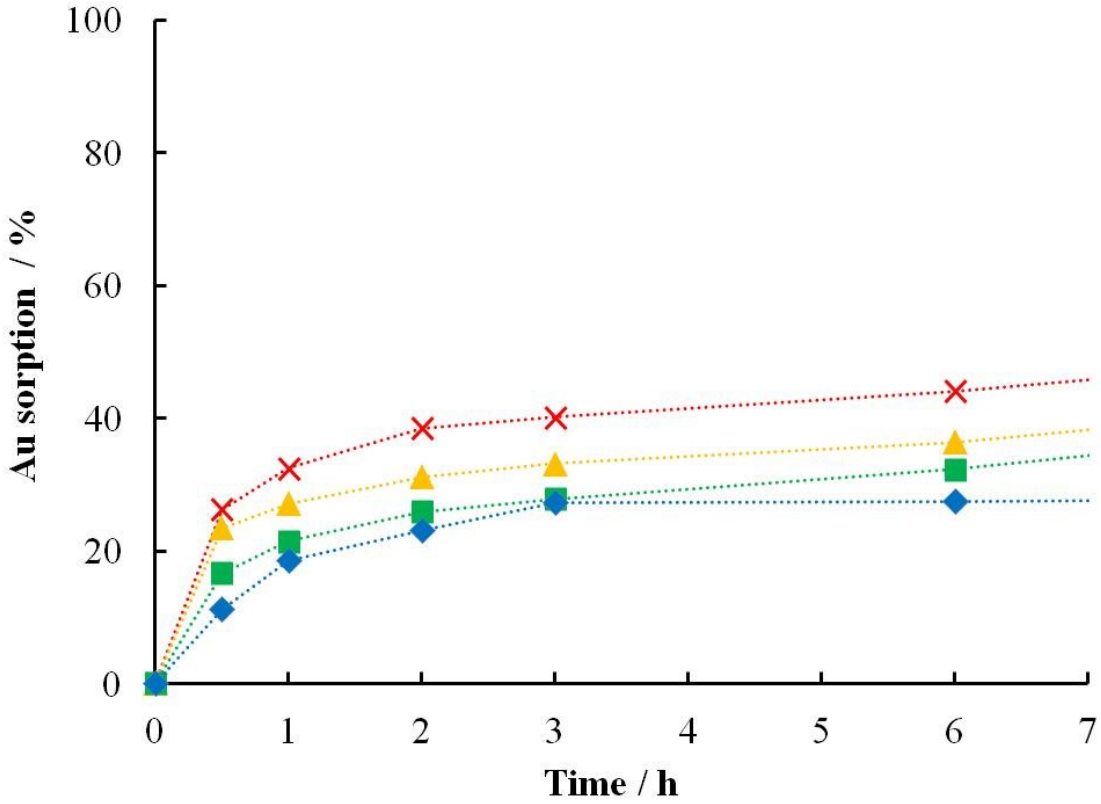

Figure III-2 Variation of % of Au sorbed with time in the presence of Pt. Initial Au concentration: 50 ppm, Initial Pt concentration: 15 ppm (×), 10 ppm(▲), 5 ppm (■), 0 ppm (◆). The amount of δ-MnO_2: 0.05 g. The volume of solution: 0.5 dm^3. pH: 8. The experiment was carried out for 6 h.

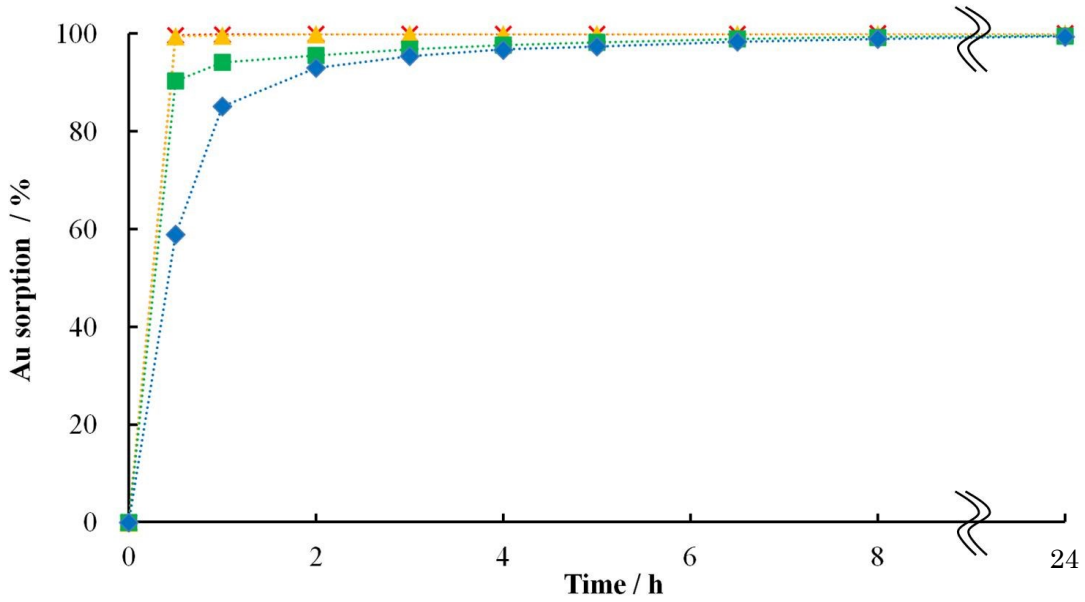

Figure III-3(a) Variation of % of Au sorbed with time in the presence of Pt. Initial Au concentration: 50 ppm, Initial Pt concentration: 100 ppm (×), 50 ppm (▲), 10 ppm (■), 0 ppm (◆). The amount of δ-MnO_2: 0.5 g. The volume of solution: 0.5 dm^3. pH: 8. The experiment was carried out for 24 h.

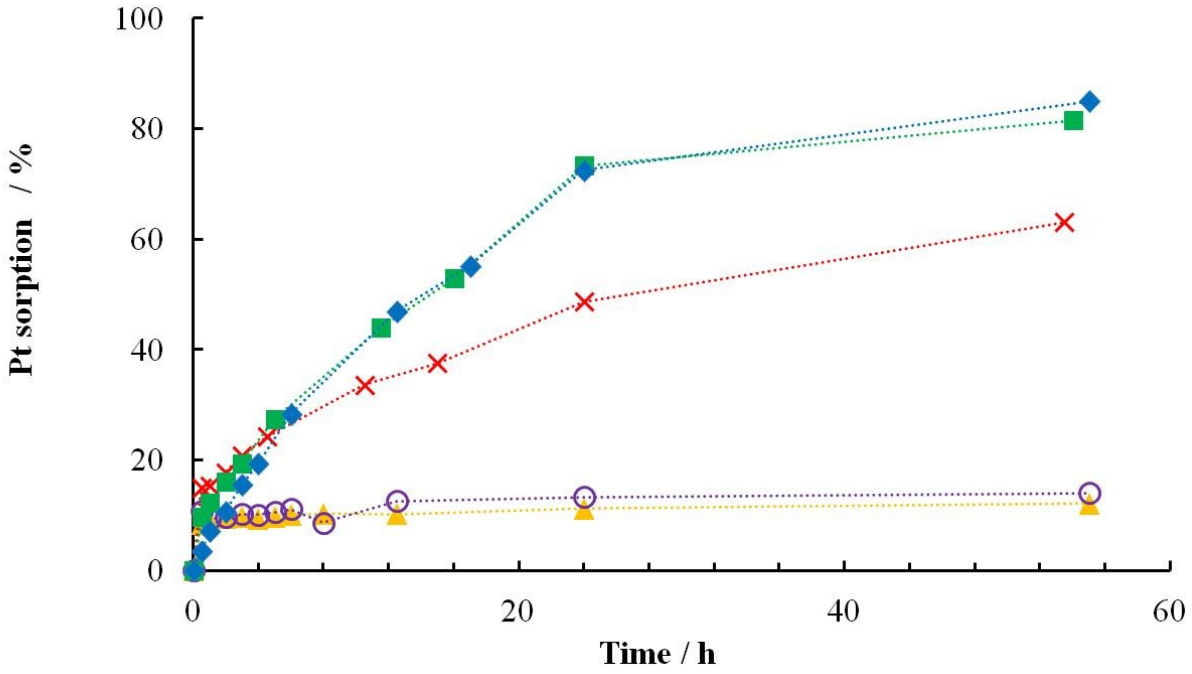

Figure III-3(b) Variation of Pt concentration with time in the presence of Au. Initial Pt concentration: 50 ppm. Initial Au concentration: 100 ppm (▲), 50 ppm (○), 25 ppm (×), 5 ppm (■), 0 ppm (◆). The amount of δ-MnO_2: 0.5 g, The volume of solution: 0.5 dm^3. pH: 8. The experiment was carried out for 54~56 h.

III-3-2 Chemical state of Au sorbed onto δ-MnO_2 by ^{197}Au Mössbauer spectroscopy

In order to examine the chemical state of Au sorbed onto δ-MnO_2, ^{197}Au Mössbauer spectra for solid samples after 24 h in the sorption experiments shown in Figs. III-3(a) and III-3(b) were measured. Figures III-4(a) and III-4(b) show the ^{197}Au Mössbauer spectra, respectively. The horizontal axis indicates the isomer shift (Doppler rate) and the vertical axis the normalized relative transmittance. The isomer shift of metallic gold (gold foil, Au(0)) is defined to be zero. Based on the isomer shift value of Au and the peak intensity, the valence state of Au and the proportion of each Au species in the solid samples can be determined (Ohashi et al., 2005). In the Figs. III-4(a) and III-4(b), two Au species were observed: Au(0) (solid line) and Au(III) (dotted line). In the both experiments, most of Au is present as Au(0), however, it should be emphasized here that when Pt(II) complex ion was absent and the initial concentration was relatively low compared with that of Au(III) complex ion (the Pt concentration is 0 and 10 ppm against the Au concentration of 50 ppm in the Fig. III-4(a) and when the Au concentration 100 ppm against the Pt concentration of 50 ppm in the Fig. III-4(b)), Au(III) species were observed, suggesting that the reduction of Au(III) complex ion sorbed onto δ-MnO_2 may be affected by Pt(II) complex ion sorbed.

III-3-3 Chemical state of Pt sorbed onto δ-MnO_2 by XAFS

In order to examine the chemical state of Pt sorbed onto δ-MnO_2, Pt L_3-edge XAFS spectra were measured. Figure III-5 shows the Pt L_3-edge XANES spectra. The first large peak, called "white line", are observed in the XANES spectra for Pt(II) and Pt(IV) standard materials and solid samples except for the standard material of Pt(0). The white line for Pt(IV) has stronger intensity than that for Pt(II) (Yamamoto and Yukumoto, 2013). From the comparison of the peak intensity, it can be definitely concluded that Pt sorbed onto δ-MnO_2 is present as Pt(IV). According to careful observation of the XANES

spectra, a small and broad peak can be seen around 11.575 keV in the XANES spectra for the Pt standard materials with Pt-Cl bond such as K_2PtCl_4 (Pt(II))and K_2PtCl_6 (Pt(IV)) (＊ in Figure III-5). Oppositely, no peak can be seen around 11.575 keV in the XANES spectra for the standard materials with Pt-O bond such as $Pt(acac)_2$ (Pt(II)) and $K_2Pt(OH)_6$ (Pt(IV)). In the XANES spectra for the solid samples, there is no peak around 11.575 keV, suggesting that Pt sorbed onto δ-MnO_2 may be coordinated by oxygen atoms. In addition, the XANES spectra for the solid samples are similar to that for $K_2Pt(OH)_6$. They are also distinguishably different from the XANES spectrum for Pt foil. Accordingly, it can be considered that Pt sorbed onto δ-MnO_2 is present as a species with $Pt(IV)O_6$ octahedral structure.

III-3-4 Redox reaction of Pt(II) and Au(III) complex anions during their competitive sorption onto δ-MnO_2

Figures III-6(a) and III-6(b) show the amounts of Au and Pt sorbed after 24 h under each experimental condition in the results shown in Figs. III-3(a) and III-3(b), respectively. The vertical axis indicates the amount (mg) of Au and Pt sorbed per one gram of δ-MnO_2. In the Fig. III-4(a), the initial coexisting Pt concentration was varied at a constant Au concentration of 50 ppm. In spite of the different Pt concentrations, all of Au were sorbed onto δ-MnO_2. While the amount of Pt sorbed into δ-MnO_2 increased with increasing the initial Pt concentration. In the Fig. III-3(b), the initial Au concentration was varied at a constant Pt concentration of 50 ppm. In the absence of Au, a significant amount of Pt was sorbed. While all of Au sorbed in spite of the initial Au concentration. The amount of Pt sorbed decreased with increasing the initial Au concentration. These results clearly indicate that the sorption affinity of Au(III) complex anion onto δ-MnO_2 is higher than that of Pt(II) complex anion.

The valence states of Au and Pt sorbed onto δ-MnO_2 are also shown in Figs. III-6(a) and III-6(b). From the result of Pt L_3-edge XANES spectra, all of the Pt sorbed existed as Pt(IV). On the other hand, Au was present as Au(0) and Au(III). The quantitative proportion of Au(0) and Au(III) can be estimated from the peak intensity ratio of ^{197}Au Mössbauer spectra and the total amount of Au and Pt sorbed onto δ-MnO_2. As described above, the amount of Au(0) increases with increasing the relative amount of Pt against Au in initial solution.

III-3-5 Simultaneous sorption mechanism of Pt(II) and Au(III) complex anions onto δ-MnO_2 by coupled redox reactions

I have published two papers about single sorption of Au(III) and Pt(II) complex ions onto δ-MnO_2 and their different redox reactions after the sorption (Yamashita et al., 2007; Chapter II in this thesis). In their sorption, the hydrolysis of Au(III) and Pt(II) complex anions is a key reaction. The Au and Pt species sorbed onto δ-MnO_2 are considered to be $[AuCl_{4-n}(OH)_n]^-$ and $[PtCl_{4-n}(OH)_n]^{2-}$ (n = 1 or 2 in seawater from the equilibrium calculation), respectively. The sorption occurs by the condensation reaction between OH^- groups of Au(III) and Pt(II) complex anions and surface OH^- groups on δ-MnO_2 to form Mn-O-Au or Mn-O-Pt bond. Although the sorption reaction is the same between Au(III) and Pt(II) complex anions as described above, the redox behavior after the sorption onto δ-MnO_2 is opposite. For the redox reaction for Au(III) sorbed onto δ-MnO_2, the structure of Au(III) complex sorbed may be distorted by the bidentate coordination and the Au(III) may be reduced to Au(0) by water molecule as shown as a following reaction (III-2), although the reducing agent was not directly confirmed (Ohashi et al., 2005).

$$Au^{3+} + 3/2H_2O \rightarrow Au(0) + 3/4O_2 + 3H^+ \qquad \text{(III-2)}$$

The bidentate coordination was confirmed by the EXAFS analysis for Au(III) complex anion sorbed on the surface of CeO_2 (unpublished data) and the subsequent spontaneous reduction reaction was also confirmed for Au(III) complex anion sorbed on the surface of alumina by AFM (unpublished data). For the redox reaction for Pt(II) complex anion sorbed onto δ-MnO_2, the Pt(II) was oxidized to Pt(IV) by Mn(IV) in δ-MnO_2 through Mn(IV)-O-Pt(II) bond. As a result, Mn(II) was released into solution. The Mn(II) released was directly detected. At pH 8, the Mn(II) hydrolyzes to form $Mn(OH)_2$ and it is easily oxidized by dissolved oxygen. Finally, the $Mn(OH)_2$ may return to δ-MnO_2 which can act as fresh sorption site. The Pt(IV) may be incorporated into the vacant site in δ-MnO_2 after the release of Mn(II) ion: the substitution of Mn(IV) with Pt(IV).

Actually, Au and Pt coexist in ocean as Au(III) and Pt(II) complex anions. Therefore, the simultaneous sorption of Au(III) and Pt(II) complex anions onto δ-MnO_2 and their redox reactions were investigated as a geochemical model reaction for elucidating the concentration mechanism of Au and Pt into marine manganese crust. In Figs. III-2, III-3 and III-6, the sorption affinity of Au onto δ-MnO_2 is higher than that of Pt. Interestingly, the reduction of Au(III) complex anion sorbed onto δ-MnO_2 is accelerated by Pt(II) complex anion sorbed. In addition, all of the Pt sorbed existed as Pt(IV). These facts clearly demonstrate that the reduction of Au(III) to Au(0) and the oxidation of Pt(II) to Pt(IV) are coupled. There is an important paper by Yamashita et al. (2008), that $Mn(OH)_2$ can rapidly reduce to Au(0). In Fig. III-6, when Pt was absent or the coexisting Pt concentration was low, the reduction of Au(III) sorbed on δ-MnO_2 was incomplete, that is, the reaction (2) (spontaneous reduction of Au(III) by H_2O) is relatively slow. However, the reduction rate increased with increasing the coexisting Pt concentration. Based on the facts in this paper and the above previous two papers (Yamashita et al., 2008; Ohashi et al., 2005), the coupled redox mechanism is proposed as shown in Fig. III-7. First

Pt(II) complex anion is sorbed by the formation of Mn(IV)-O-Pt(II) bond. Two electrons are transferred from Pt(II) to Mn(IV). As a result, Pt(II) is oxidized to Pt(IV), on the other hand, Mn(IV) is reduced to Mn(II). The Mn(II) is rapidly hydrolyzed to form $Mn(OH)_2$ under pH 8 (in seawater). The $Mn(OH)_2$ can immediately reduce Au(III) complex anion sorbed onto δ-MnO_2 to Au(0). By this reduction reaction of Au(III), $Mn(OH)_2$ is effectively oxidized and converted to δ-MnO_2 which can act as fresh sorption sites for Au(III) and Pt(II). These reactions can be represented as follows.

$$3Pt^{2+} + 3Mn^{4+} \text{ (in } \delta\text{-}MnO_2) \rightarrow 3Pt^{4+} + 3Mn^{2+} \qquad \text{(III-3)}$$

$$3Mn^{2+} + 6H_2O \rightarrow 3Mn(OH)_2 + 6H^+ \qquad \text{(III-4)}$$

$$3Mn(OH)_2 + 2Au^{3+} \rightarrow 3MnO_2 \text{ (as } \delta\text{-}MnO_2) + 2Au(0) + 6H^+ \qquad \text{(III-5)}$$

As proposed above, the efficient redox cycle of Pt(II) and Au(III) is possible to be built up during the growth process of marine manganese crust. Although the reaction (III-2) (spontaneous reduction of Au(III)) may occur on δ-MnO_2, it is significantly slower than the reactions (III-3) - (III-5).

If gold is present as Au(I) complex ion in seawater, it disproportionates into Au(0) and Au(III) after the sorption (Yonezu et al., 2007). The Au(III) can be reduced to Au(0) by the above reaction after the sorption by δ-MnO_2.

This is a new concentration mechanism of both Au and Pt into marine manganese crust. This mechanism is a important information on consideration of geochemical circulation of Au and Pt including their uptake by marine manganese crust.

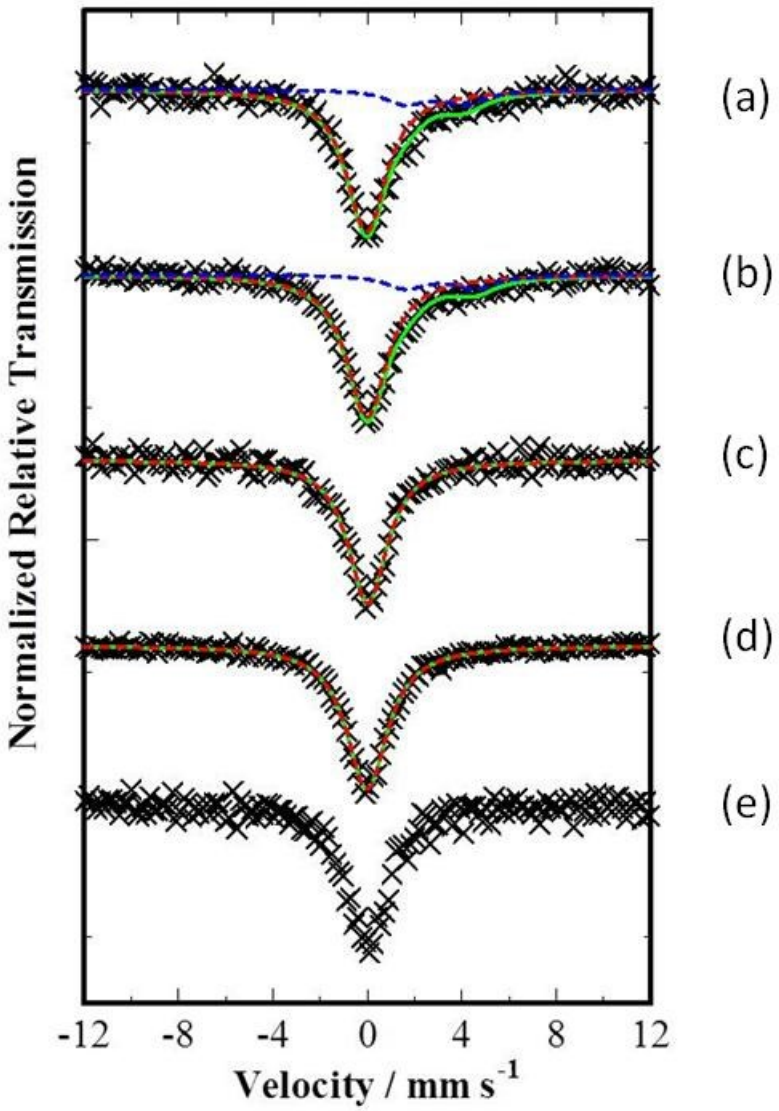

Figure III-4(a) ^{197}Au Mössbauer spectra for solid samples and Au foil as a standard material. Samples are obtained from the experiments shown in Fig. III-3(a). Initial Au concentration: 50 ppm. Initial Pt concentration: (a) 0 ppm, (b) 10 ppm, (c) 50 ppm, (d) 100 ppm. Standard material Au foil (e). Reaction time: 24 h.

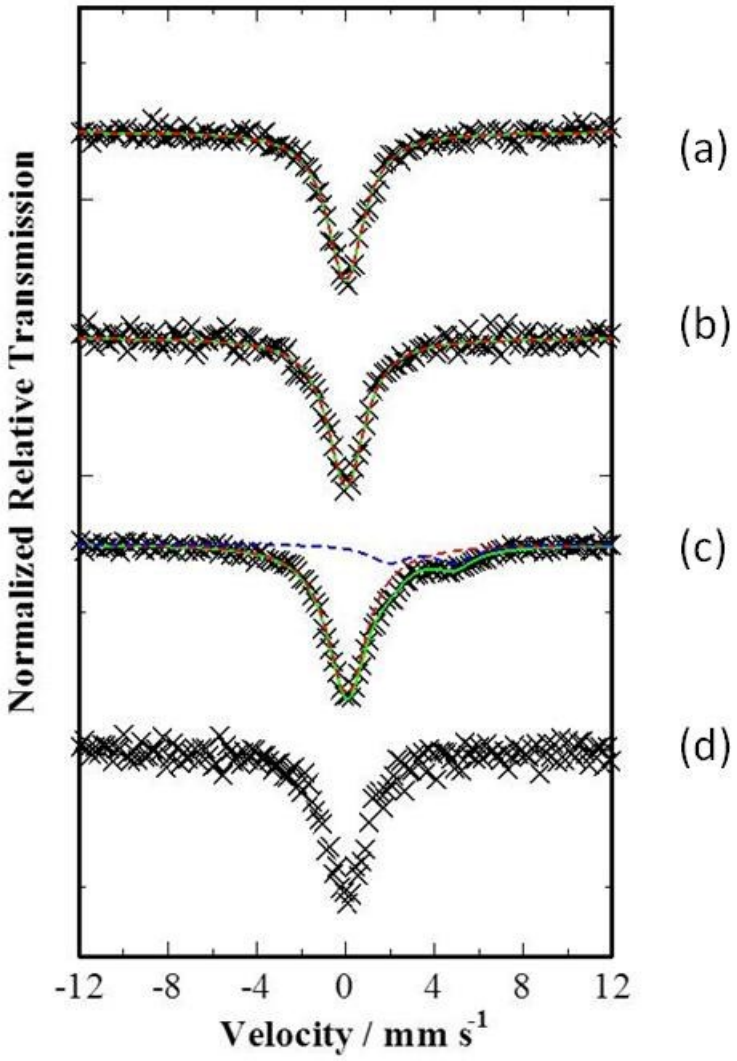

Figure III-4(b) ^{197}Au Mössbauer spectra for solid samples and Au foil as a standard material. Samples are obtained from the experiments shown in Fig. III-3(b). Initial Pt concentration: 50 ppm. Initial Au concentration: (a) 5 ppm, (b) 25 ppm, (c) 100 ppm. Standard material Au foil (d). Reaction time: 24 h.

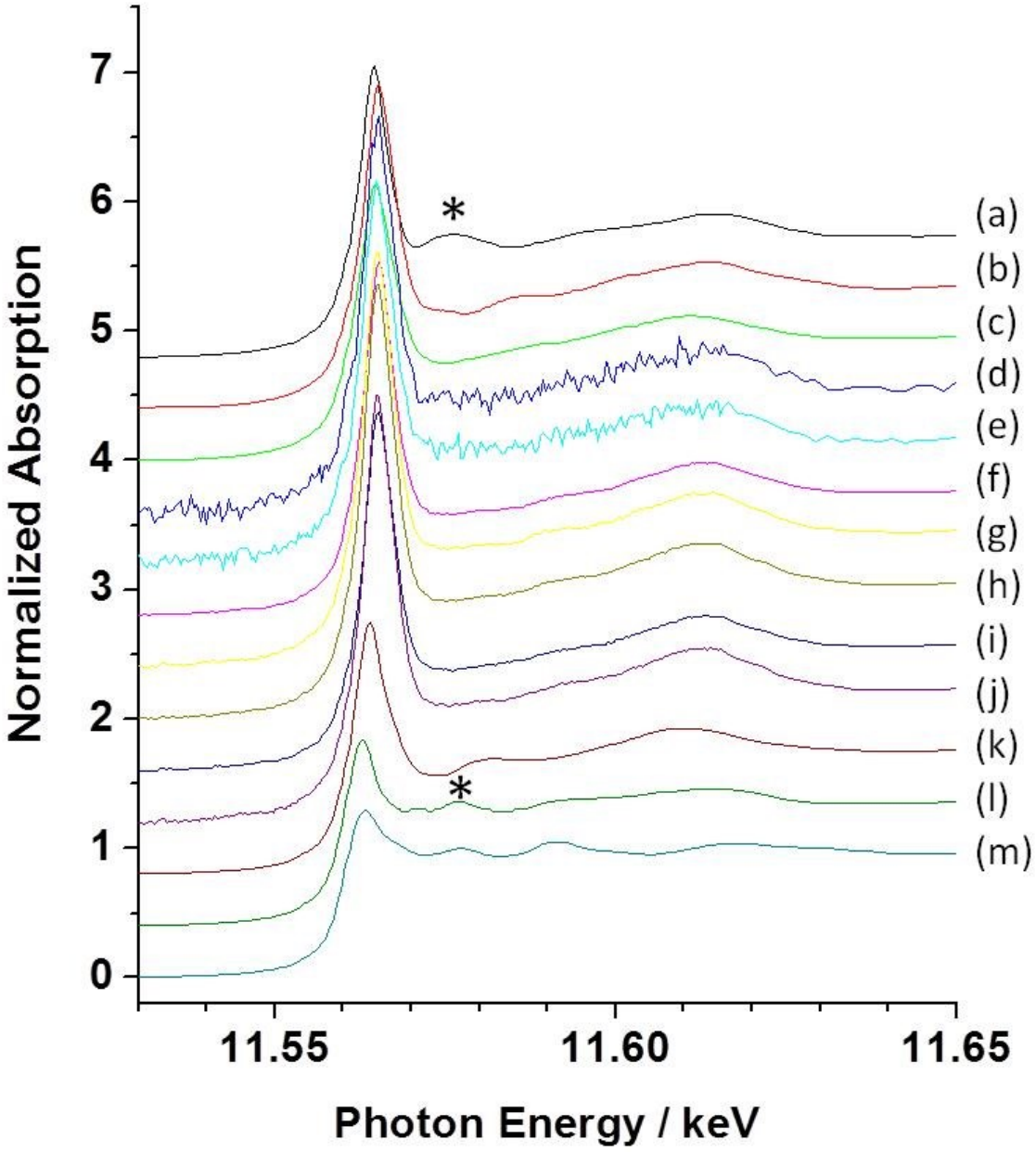

Figure III-5 Pt L_3 - edge XANES spectra for solid samples (d) ~ (j) and standard materials (a) ~ (c) and (k) ~ (m). (a)K_2PtCl_6, (b)Na_2PtOH_6, (c) PtO_2, (d) 10 ppm Pt,50 ppm Au (e) 50 ppm Pt,100 ppm Au, (f) 50 ppm Pt,50 ppm Au, (g) 50 ppm Pt,25 ppm Au, (h) 50 ppm Pt,5 ppm Au,(i) 50 ppm Pt,0 ppm Au, (j) 100 ppm Pt,50 ppm Au, (k) $Pt(acac)_2$, (l) K_2PtCl_4 (m) Pt foil. Peak at 11.575 keV appeared for Pt standard materials with Pt-Cl bonds. No peak appeared around 11.575 keV for standard materials with Pt-O bonds and the solid samples (Pt sorbed onto δ-MnO_2). The solid samples were obtained from the experiment shown in Fig. III-3. Reaction time: 24 h.

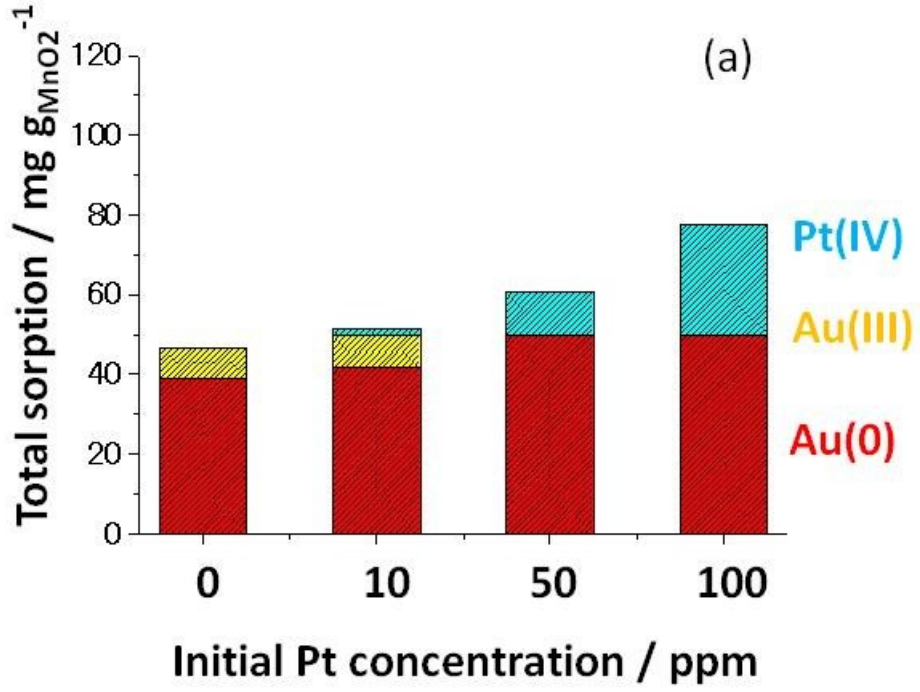

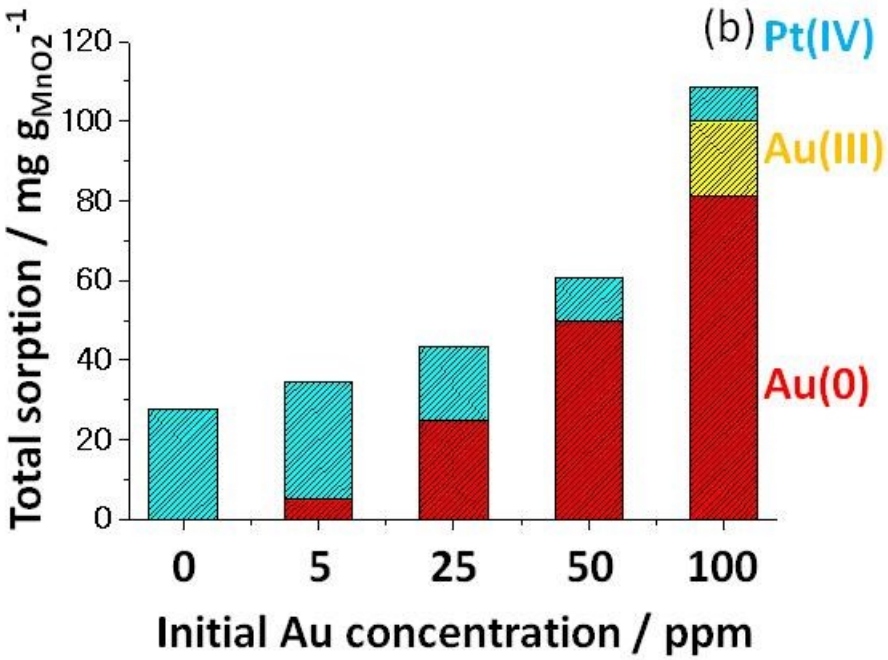

Figure III-6(a) Variation of the amount of Au and Pt sorbed and the valence state with initial Pt concentration. Data at 24 h shown in Fig. III-3(a) are represented. Initial Au concentration: 50ppm.

Figure III-6(b) Variation of the amount of Au and Pt sorbed and the valence state with initial Au concentration. Data at 24 h shown in Fig. III-3(b) are represented. Initial Pt concentration: 50ppm.

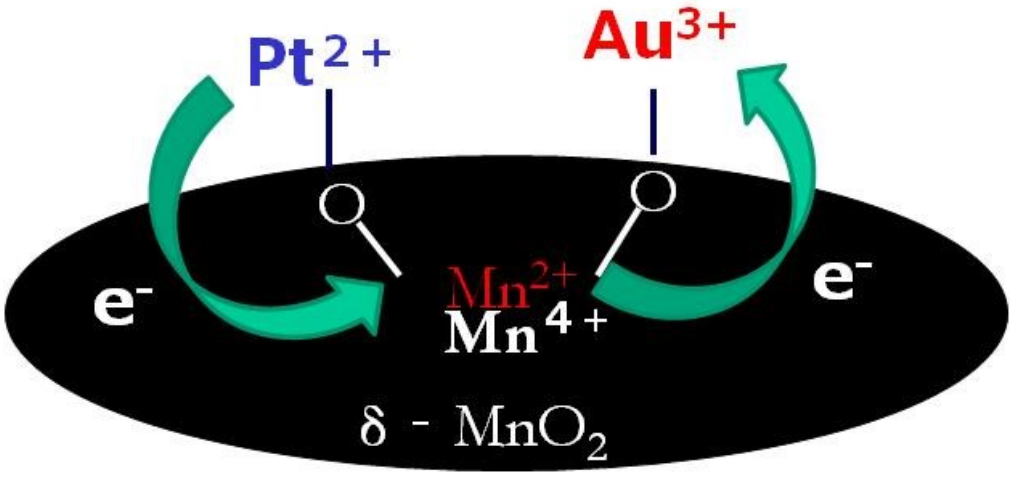

Figure III-7 A proposed simultaneous sorption mechanism of Au and Pt onto δ-MnO_2 and the coupled redox reaction. Green arrows indicate the transfer of two electrons: Pt(II) → Mn(IV) and Mn(II) → Au(III).

References

Halbach P. (1984) Deep-sea metallic deposits. *Ocean Management* **9**: 35-60

Halbach P. (1986) Process controlling the heavy metal contribution in Pacific ferromanganese nodules and crusts. *Geol. Rundsch.* **75** : 235-247.

Halbach P., Kriete C., Prause B. and Puteanus D. (1989) Mechanisms to explain the platinum concentration in ferromanganese seamount crusts. *Chem. Geol.* **76**: 95-106.

Hein J. R., Mizell K., Koschinsky and Tracey A. (2013) Conrad Deep-ocean mineral deposits as a source of critical metals for high- and green-technology applications: Comparison with land-based resources. *Ore Geology Reviews* **51**: 1-14.

Hodge V. F., Stallard M., Koide M. and Goldberg E. D. (1985) Platinum and the platinum anomaly in the marine environment. *Earth Planet. Sci. Lett.* **72**: 158-162.

Koide M, Hodge V F, Yang J S, Stallard M and Goldberg E G, (1986) Some comparative marine chemistries of rhenium, gold, silver and molybdenum. *Appl. Geochem.* **1** : 705-714.

Nozaki Y. (1992) Trace elements in sea water: Their mean concentrations and North Pacific profiles. *Chikyukagau (Geochemistry)* **26**: 25-39.

Ohashi H., Ezoe H., Yamashige H., Okaue Y., Matuo S., Kurisaki T., Wakita H. and Yokoyama T. (2005) Reduction behavior of Au(III) complex ions sorbed on the surface of manganese dioxide: XPS study. Adv. *X-Ray Chem. Anal. Jpn.* **36**: 339-345.

Ravel B. and Newville J. M. (2005) ATHENA, ARTEMIS, HEPHAESTUS: data analysis for X-ray absorption spectroscopy using IFEFFIT. *Synchrotron Rad.* **12**: 537-541.

Terashima S., Usui A., Nakao S. and Mita N. (1989) Geochemistry of platinum and gold in ocean-floor ferromanganese crusts and nodules. *Bull. Geol. Surv. Japan* **40**: 127-141.

Takematsu N. (1998) Manganese nodule: Its formation mechanism and role. *Kouseishakouseikaku Co., Ltd., Japan*.

Terashima S., Usui A., Nakao S. and Mita N. (1989) Geochemistry of platinum and gold in ocean-floor ferromanganese crusts and nodules. *Bull. Geol. Surv. Japan* **40**: 127-141.

Usui A. (2010) "Mineral resources of the seabed", *Ohmsha.*

Yamashita M., Ohashi H., Kobayashi Y., Okaue Y., Kurisaki T., Wakita H. and Yokoyama T. (2008) Coprecipitation of gold(III) complex ions with manganese(II) hydroxide and their stoichiometric reduction to atomic gold (Au(0)): Analysis by Mössbauer spectroscopy and XPS. *J. Colloid Interface Sci.* **319**: 25–29.

Yamamoto T. and Yukumoto A. (2013) Apparent Chemical Shifts at X-ray Absorption Edges of 3d-, 4f-, 5d- and 5p-elements for Empirical Chemical State Analysis. *Bunseki Kagaku*. **62**: 555-563.

Yonezu K., Yokoyama T., Okaue Y., Imai A. and Watanabe K. (2007) Concentration of Gold(I) Thiosulfate Complex Ions on the Surface of Alumina Gel and their Change in Chemical State: Preliminary Experiment in the Elucidation of the Formation Mechanism of Epithermal Gold Deposits. *Resource Geology.* **57**: 400-408.

Chapter IV
Conclusion and geochemical implication

The formation mechanism of marine ferromanganese nodule and crust is divided into three categories: (1) hydrogenous origin, (2) diagenetic origin, and (3) hydrothermal origin. Although the ferromanganese nodule and crust consist of the mixture of hydrous ferric and manganese(IV) oxides, the Mn/Fe atomic ratio is dependent on the formation conditions. Since the ferromanganese nodule and crust play an important role as a sink of trace elements in ocean, that is, they concentrate the trace elements from seawater compared to their contents in the earth crust, it is interesting geochemical samples to elucidate the circulation of trace elements on the surface of earth including chemical weathering of rocks, dissolution of trace elements into river water, transport of trace elements by river water into ocean, and their uptake by ferromanganese nodule and crust. Interestingly, it has been found that cobalt and platinum are highly concentrated in the marine ferromanganese crust which covers around the top of seamount. The uptake mechanism of trace elements by the marine ferromanganese crust has been interpreted by “electrochemical model”. According to the model, cations such as Cu(II) and Ni(II) present in seawater are sorbed onto sinking particles of MnO_2 with negative charged on the surface in seawater (around pH 8), whereas oxoanions such as $[MoO_4]^{2-}$, CrO_4^{2-} are sorbed onto sinking particles of FeOOH with positive charges on the surface in seawater. The ferromanganese nodule and crust are formed by the sedimentation of the particles on the seabed.

However, Usui et al. (1989) reported that the Pt content moderately correlated with the content of Mn for the marine ferromanganese nodule and crust collected at both the Ogasawara Plateau ($r = 0.55$) and the Antarctic Ocean ($r = 0.66$). Although Pt has been considered to be present as $[PtCl_{4-n}(OH)_n]^{2-}$ complex anion, specically Pt may be sorbed by

MnO_2 particles (vanadite (δ-MnO_2)). It indicates that there is another sorption mechanism which cannot be explained by the electrochemical model. For the sorption mechanism of Pt into marine ferromanganese nodule and crust, two different ideas have been proposed: Pt(II) is sorbed as Pt(0) or Pt(IV). However, a reasonable and chemical explanation has not been done yet. Therefore, in order to elucidate the sorption mechanism of Au and Pt by marine ferromanganese crust, I have investigated the sorption of Au and Pt complex anions by δ-MnO_2 in this thesis. In this thesis two kinds of investigations were conducted: (1) the sorption behavior of Pt(II) complex anions onto δ-MnO_2 and (2) simultaneous sorption behavior of Au(III) and Pt(II) complex anions onto δ-MnO_2.

Figure IV-1 shows the electrochemical model (a) and the specific sorption mechanism of Au and Pt (b). In Fig. II-2 in this thesis, Pt(II) complex anion was confirmed to be present as $[PtCl_{4-n}(OH)_n]^{2-}$. These hydrolyzed Pt(II) complex anions were sorbed on δ-MnO_2 by overcoming the electrostatic repulsion between negative charges on the surface of δ-MnO_2 and negative charges of Pt(II) complex anion and the Mn-O-Pt bond may be formed (chemical sorption). In addition, after the sorption of Pt(II) complex anion, the Pt(II) was oxidized to Pt(IV) by Mn(IV) in δ-MnO_2. Platinum is considered to be concentrated into marine ferromanganese crust by the above same mechanism. Since Pt(IV) and Mn(IV) have the same valence state, same coordination structure and the close ionic radius are close (Pt(IV), 0.60 Å and Mn(IV), 0.54 Å), they are possible to substitute, that is, the isomorphous substitution occurs between Pt(IV) and Mn(IV).

From the statistic analysis, there is a positive correlation between the contents of Au and Pt in marine ferromanganese nodule and crust. The fact suggests that the sorption behavior of Au and Pt onto marine ferromanganese nodule and crust may be coupled. In addition, Ohashi et al. (2005) reported that Au is present as $[AuCl_{4-n}(OH)_n]^-$ in solution

and it can be sorbed rapidly and significantly on δ-MnO_2 to form Mn-O-Au bond. After the sorption, the Au(III) complex anions were reduced spontaneously to Au(0). Consequently, Au(III) and Pt(II) complex ions sorbed to δ-MnO_2 show the opposite redox reactions. In ocean, Au and Pt concentrations are roughly close. Therefore, Au and Pt may be sorbed at the same time. In their sorption process to marine ferromanganese crust, whether their redox reaction is coupled or not is interesting in geochemistry.

According to the result in Chapter III in this thesis, first Pt(II) complex anion is sorbed by the formation of Mn(IV)-O-Pt(II) bond as shown in Fig. IV-1(b). Two electrons are transferred from Pt(II) to Mn(IV). As a result, Pt(II) is oxidized to Pt(IV), on the other hand, Mn(IV) is reduced to Mn(II) as shown in Fig. IV-2. The Mn(II) is rapidly hydrolyzed to form $Mn(OH)_2$ under pH 8 (in seawater). The $Mn(OH)_2$ can immediately reduce Au(III) complex anion sorbed onto δ-MnO_2 to Au(0). By this reduction reaction of Au(III), $Mn(OH)_2$ is effectively oxidized to δ-MnO_2 which can act as fresh sorption sites for Pt(II). These reactions can be represented as follows.

$$3Pt^{2+} + 3Mn^{4+}\ (\text{in } \delta\text{-}MnO_2) \rightarrow 3Pt^{4+} + 3Mn^{2+} \qquad \text{(IV-1)}$$

$$3Mn^{2+} + 6H_2O \rightarrow 3Mn(OH)_2 + 3H^+ \qquad \text{(IV-2)}$$

$$3Mn(OH)_2 + 2Au^{3+} \rightarrow 3MnO_2\ (\text{as } \delta\text{-}MnO_2) + 2Au(0) + 6H^+ \qquad \text{(IV-3)}$$

This is a new concept for the concentration mechanism of both Au and Pt into marine manganese crust. This mechanism is an important information on consideration of geochemical circulation of Au and Pt including their uptake by marine ferromanganese crust.

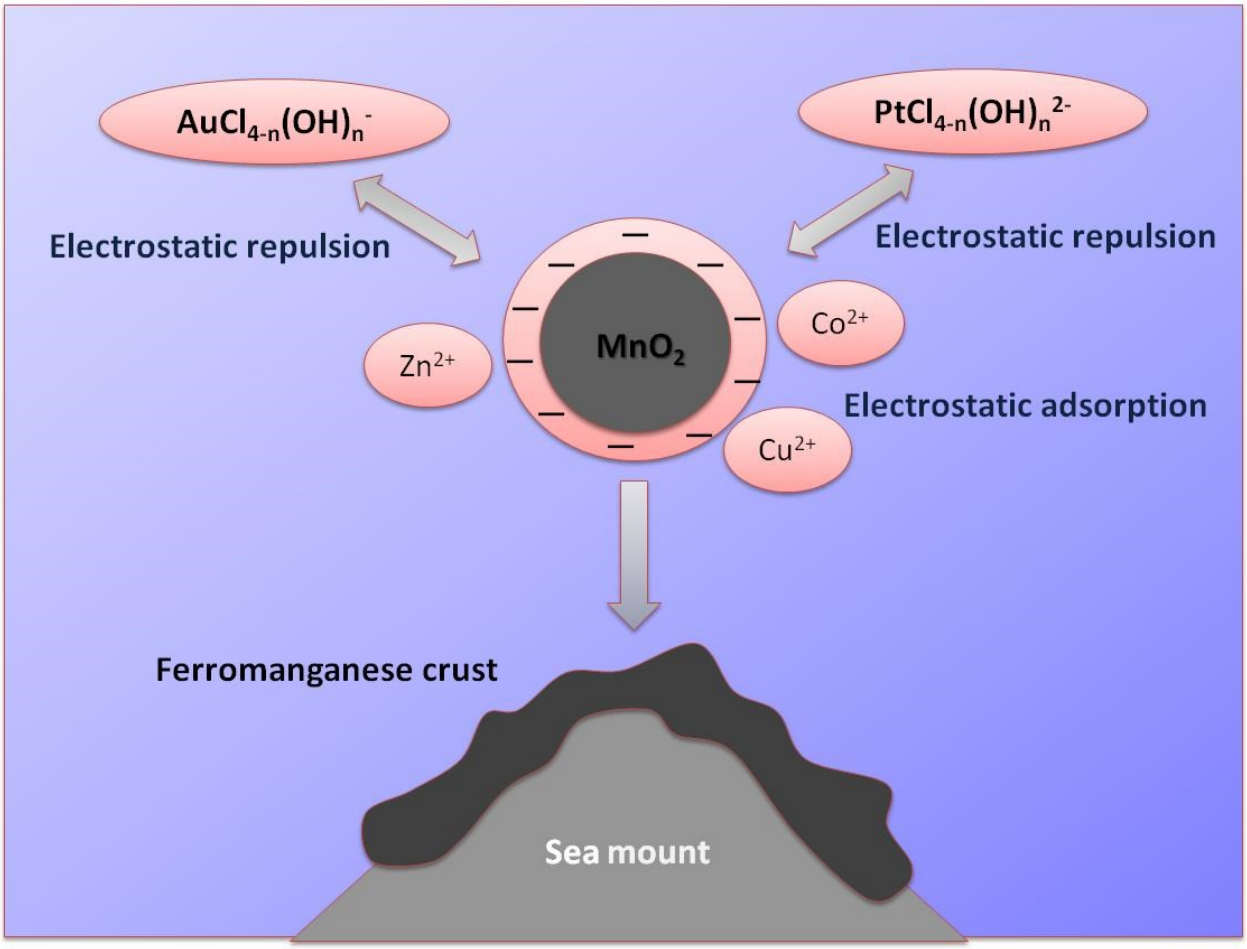

Figure IV-1(a) The electrochemical model for the interaction between trace elements in seawater and manganese dioxide particle.

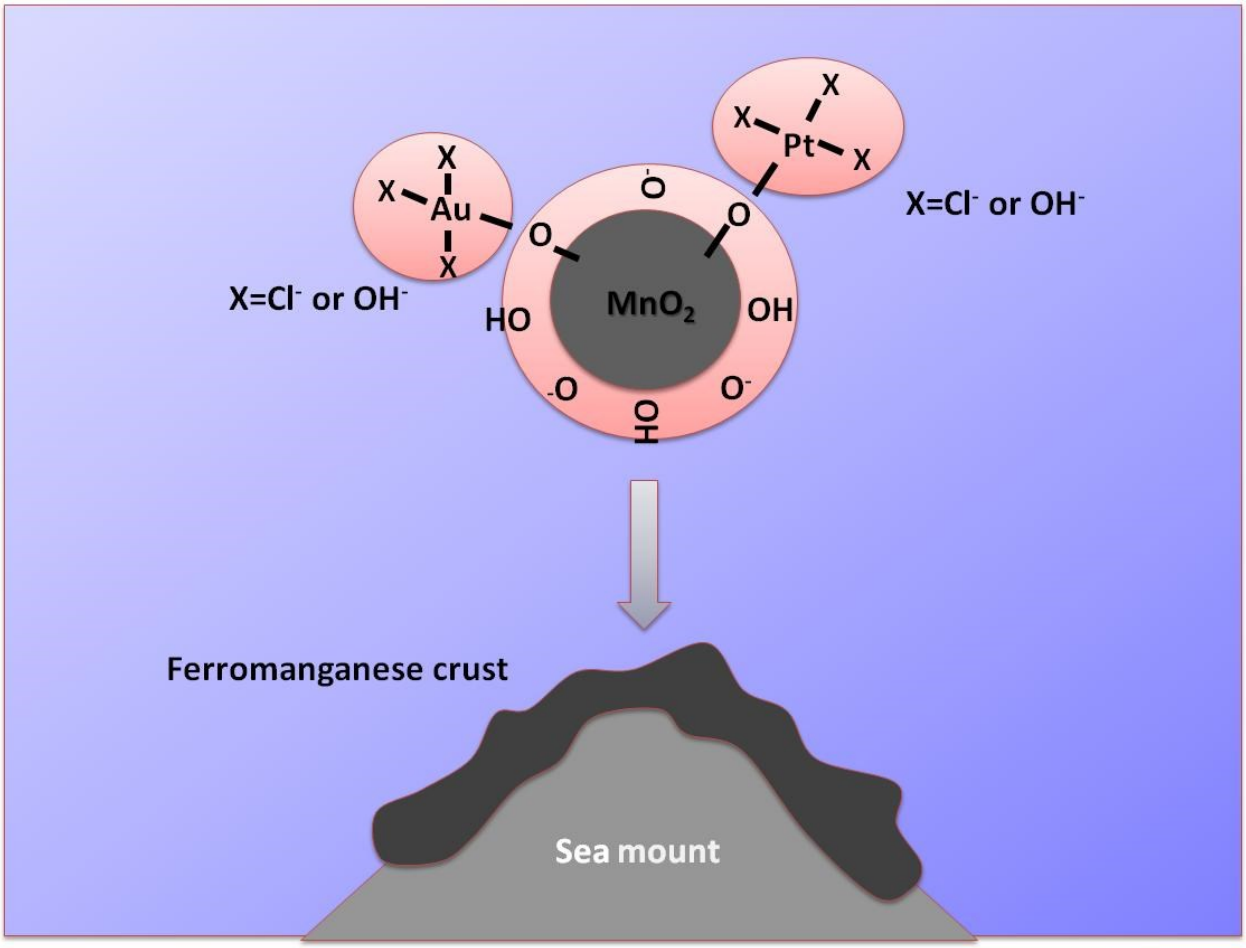

Figure IV-1(b) Sorption model of Pt and Au onto marine ferromanganese crust due to the formation of Mn(IV)-O-Pt(II) and Mn(IV)-O-Au(III) bonds by overcoming the electrostatic repulsions.

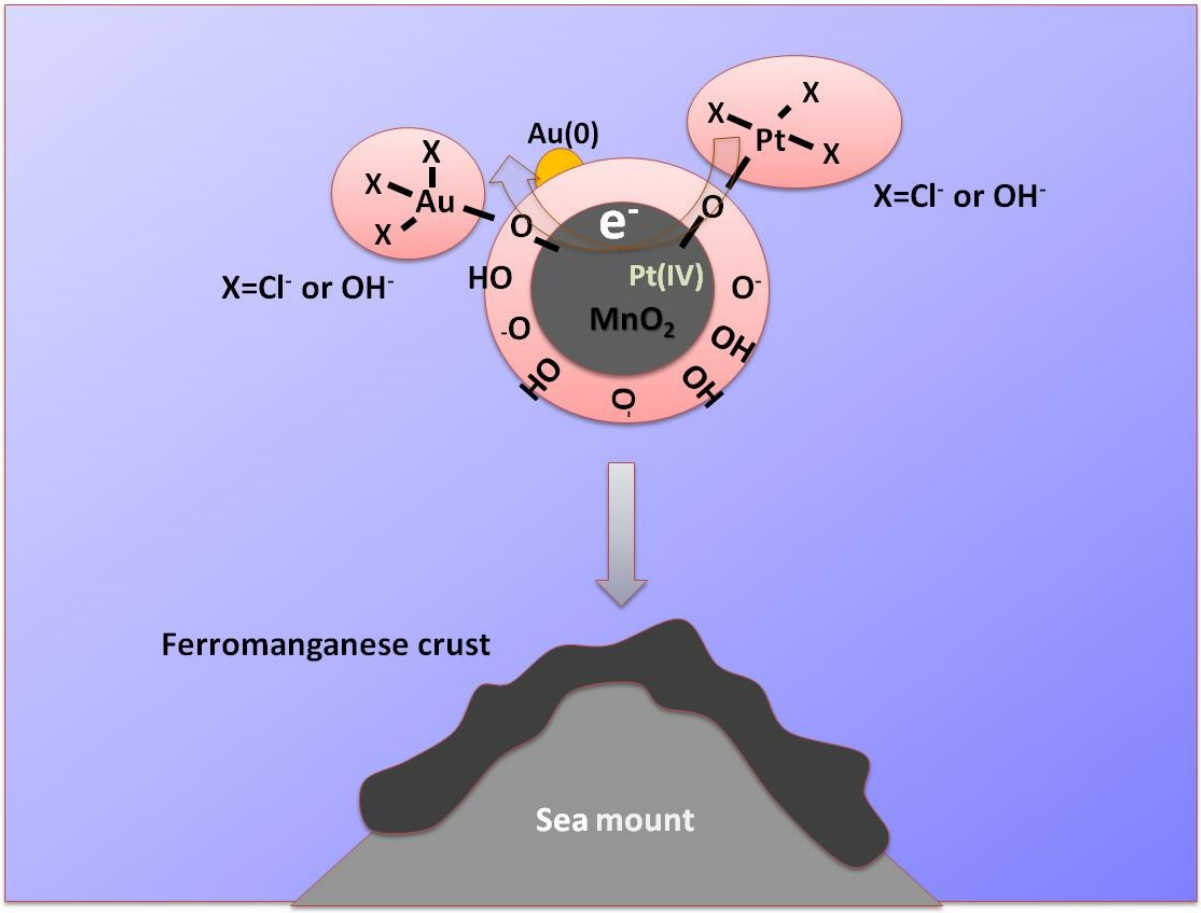

Figure IV-2 A coupled redox model of Pt and Au sorbed to marine ferromanganese crust. The arrow indicate the transfer of electrons.

References

Ohashi H., Ezoe H., Yamashige H., Okaue Y., Matuo S., Kurisaki T., Wakita H. and Yokoyama T. (2005) Reduction behavior of Au(III) complex ions sorbed on the surface of manganese dioxide: XPS study. Adv. *X-Ray Chem. Anal. Jpn.* **36**: 339-345.

Usui A., Mellin T., Nohara M. and Yuasa M. (1989) Structure stability of marine 10 Å manganese from the Ogasawara (Bonin) Arc: Implications for low-temperature activity. *Mar.Geol.* **86**: 1-56.

Acknowledgements

I would like to thank Prof. Takushi Yokoyama who has taught me over long years. I would like to thank Associate Prof. Satoshi Utsunomiya and Lecturer Yoshihiro Okaue for their advices throughout this work. I'm also grateful to Assistant Prof. Hironori Ohashi for their advices throughout this work and for their support of the XAFS study. I'm also grateful to all the members of the Inorganic Reaction Chemistry laboratory support to my collage life.

In Kyuden Sangyo Co. INC, I'm deeply grateful to Department-director Dr. Yukio Imaizumi, Group manager Dr. Tatsuto Iwanaga and Dr. Masami Noto for their liberal support.

I thank Prof. Yoshio Takahashi (Hiroshima University) for helping the measurements of XAFS and the analysis of the EXAFS spectra. And I also thank Assistant Prof. Yasuhiro Kobayashi (Kyoto University) for helping the measurements of Mössbauer spectroscopy. XPS was measured at the Center of Advanced Instrumental Analysis, Kyushu University, Fukuoka, Japan. This study was financially supported by The Japan Mining Promotive Foundation (2008~2010) and by JST-CREST, JST Research for Promoting Technological Seeds.

Finally I would also like to express my gratitude to my grandfather, grandmother, mother, and my husband for their generous support and warm encouragements.